

AD-A280 815



15 June 1994.

MEMORANDUM FOR RECORD

SUBJECT: Master's Thesis Security Classification

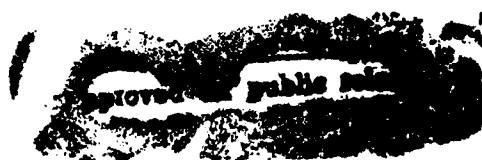
1. Reference: Student Handbook, U.S. Army Student Detachment, 6 June 1991.
2. The enclosed master's thesis document, titled "Intensity Calibration for Raman Multichannel Spectrometers", is unclassified and releasable to the public.

Enclosure

Juan A. Cuadrado
Juan A. Cuadrado
Captain , CM

DTIC
ELECTE
JUN 28 1994
S G D

94-19572



94 6 27

THE FLORIDA STATE UNIVERSITY
COLLEGE OF ARTS AND SCIENCES

**INTENSITY CALIBRATION FOR RAMAN MULTICHANNEL
SPECTROMETERS**

By
JUAN ARIEL CUADRADO REYES

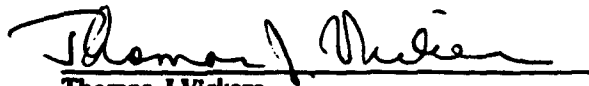
A Thesis submitted to the
Department of Chemistry
in partial fulfillment of the
requirements for the degree of
Master of Science

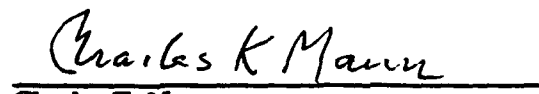
Degree Awarded:
Summer Semester, 1994

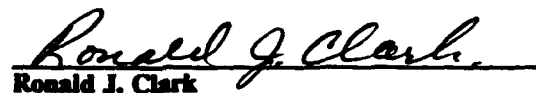
Accession For	
NTIS CRA&I	<input checked="checked" type="checkbox"/>
DTIC TAB	<input type="checkbox"/>
Unannounced	<input type="checkbox"/>
Justification	
By	
Distribution /	
Availability Codes	
Dist	Avail and/or Special
A-1	

DTIC QUALITY INSPECTED 8

The members of the Committee approve the thesis of
Juan Ariel Cuadrado Reyes defended on June 6, 1994.


Thomas J. Vickers
Professor Directing Thesis


Charles K. Mann
Committee Member


Ronald J. Clark
Committee Member

To Ada Nelia ---

*For a beautiful childhood together, since 18 years ago , and for a lifetime of love
and unconditional friendship now and forever!*

Acknowledgments

This work is the result of the combined efforts of many special individuals that I would like to recognize at this time. I am grateful to professors Thomas J. Vickers and Charles K. Mann for accepting me as part of their dynamic research team and for providing me with their supporting leadership every step of the research. My thanks to the U.S. Army and U.S. Military Academy for the opportunity to attend graduate school and their support for these last two years.

I would like to thank Captain Augustus W. Fountain, Dr. Ching-Hui Tseng, Bin Sun, Daniel Lombardi, and Joseph Ford for their support and advice in the multiple experimentation phases of this research. My special thanks to Magdalena I. Ivanova for her critical assistance on the final stages of the thesis write-up and for her sound recommendations.

My deepest thanks to my beloved wife Ada Nelia for her unconditional support every step of the way. In fact, this is not just my accomplishment, but hers. Ada, also a chemist, was careful enough to don't embarrass me, when I missed the point, while she kindly point me out in the right direction when it was required. Her faith on our success and her strong will kept us ready to stand this challenge and any others to come!

Table of Contents

LIST OF TABLES	vii
LIST OF FIGURES	viii
ABSTRACT	x
1 INTRODUCTION	1
1.1 Multichannel Spectrometers and Array Detectors	1
1.2 Standard Method to Correct Sensitivity Variations	2
1.3 Development of a New Method for Sensitivity Correction	4
2 CALIBRATION TRANSFER FROM THE STANDARD OF SPECTRAL RADIANCE TO THE LABORATORY WORKING STANDARD WHITE LIGHT SOURCE	5
2.1 Introduction	5
2.1.1 Problem Statement	5
2.1.2 The Proposed Solution	6
2.1.3 The Scope	7
2.2 Theoretical Background	8
2.2.1 Sampling Geometry Control	8
2.2.2 Spectral Radiance Sources	10
2.2.3 Fiber - Optic Probes	15
2.2.4 Definition of Theoretical Parameters	23
2.3 EXPERIMENTAL	27
2.3.1 Calibration Transfer General Steps	27
2.3.2 Instrumentation	30
2.3.3 Measurements	36
2.4 Results and Discussion	37
2.4.1 Polynomial Equation for the Shelf Standard Source	37
2.4.2 White Light Source Holders	41
2.4.3 True Spectrum of the Laboratory Working Standard White Light Source	45
2.5 Conclusions	54
3 SENSITIVITY CORRECTION FOR MULTICHANNEL SPECTROMETERS	56
3.1 Introduction	56
3.2 Experimental	57

3.2.1 Outline of Experimental Procedure . . .	57
3.2.2 Sample Materials	58
3.2.3 Instrumentation	58
3.2.4 Measurements	60
3.3 Results and Discussion	61
3.3.1 Acetonitrile Tests	61
3.3.2 Quinine Fluorescence Spectrum Test . .	70
3.3.3 Conclusions	72
4 GENERAL CONCLUSIONS AND RECOMMENDATIONS FOR THE INTENSITY CALIBRATION OF RAMAN MULTICHANNEL SPECTROMETERS	77
4.1 General Conclusions	77
4.2 Recommendations	80
REFERENCES	84
BIOGRAPHICAL SKETCH	85

List of Tables

2.1	Theoretical Output of EPT1109 Standard of Spectral Radiance and Fiber-Optic Probe (1x1) at 100 cm Separation.	38
2.2	Theoretical Output of EPT1109 Standard of Spectral Radiance and Fiber-Optic Probe (1x1); 50 cm Separation.	41
2.3	Coefficients for the Equation Describing the Curve LAB $F_{\lambda p}$ Versus λ	54
3.1	Spectral Windows For Peak Ratios of Acetonitrile.	64
3.2	Results From Peak Intensity Ratio Comparison Between Dispersive Raman With and Without White Light Correction and FT-Raman.	67

List of Figures

2.1	Arrangement of External Optics to Focus the Image of the Tungsten Filament at the Entrance of the Radiometer	12
2.2	Important Parameters to Match the Fiber-Optic Probe With the Spectrometer.	17
2.3	Filling the Entrance Slit of the Spectrometer with the Magnified Image.	18
2.4	1X6 Configuration of Fiber-Optic Probe.	19
2.5	Overlapping Cones Area of 1X1 Fiber-Optic Probe.	20
2.6	Area of the Filament Defined by the Magnified Image and the Spectrometer's Slit.	25
2.7	Magnification of the Filament Image's Width and Height	25
2.8	Dispersive-Raman System with Fiber-Optic Probe and CCD Detector.	30
2.9	Schematic of the Shelf and Laboratory Working Standard White light Sources.	31
2.10	Current Laboratory Working Standard White Light Source Holder.	33
2.11	Shelf Standard White Light Source Holder 1.	34
2.12	Shelf Standard White Light Source Holder 2.	35
2.13	Plot of the Theoretical Output of EPT1109 Standard of Spectral Radiance and Fiber-Optic Probe at 100 cm Separation.	39
2.14	Plot of the Theoretical Output of EPT1109 Standard Spectral Radiance and Fiber-Optic Probe(1x1) at 50 cm Separation	40

2.15	Initial Model of the Laboratory Standard White Light Source Holder	42
2.16	Plot of the Calculated Intensity for the Central Wavelength, in Counts/Seconds, of Each Window Versus Wavelength, in Angstroms	50
2.17	Plot of LAB $F_{\lambda W}$ and SHELF $F_{\lambda W}$ Versus Wavelength for the Central Wavelength of Each Window.	52
2.18	Plot of LAB $F_{\lambda P}$, in Photons/seconds Angstroms, Versus Wavelength.	53
3.1	Varian Spectrofluorometer, SF330.	59
3.2	Experimental Arrangement for the Measurement of the Quinine Fluorescence Spectrum with a Fiber-Optic Probe.	61
3.3	True Output of the Laboratory Standard White Light Source with the 1x1 Fiber-Optic Probe.	62
3.4	Acetonitrile Spectrum, Window 6, from Raw to White Light Corrected Spectrum.	63
3.5	Acetonitrile Spectrum After Subtraction of KCl Spectrum; Window 6.	65
3.6	Acetonitrile FT-Raman Spectrum.	66
3.7	Quinine Fluorescence Spectrum Based on Splines Intensities.	71
3.8	Comparison of Quinine Fluorescence Spectra; Spline Calculations, Hamaguchi's Version, and Spline of NIST SRM 936.	73
3.9	Quinine Fluorescence Spectrum According to W. H. Melhuish [10].	74

Abstract

Multichannel spectrometers have been important in the recent development of Raman and other types of spectroscopy. The array detectors used in multichannel spectrometers have raised several technical problems together with the advantages that these detectors offer over single channel spectrometers. An adequate sensitivity calibration is among the most challenging problems . A calibrated white light source is required to correct both channel-to-channel sensitivity variations and the variations of each channel with wavelength.

Several attempts to solve these problems have been made, but present methods are either too tedious to do in routine operations or they only correct sensitivity variations within a spectral window. These last methods do not allow for smooth connection of several spectral windows to obtain a whole spectrum for a given compound.

We will report our findings on a new suitable and reliable laboratory white light source and correction method for multichannel spectrometers. A discussion in depth of the calibration transfer from the National Institute of Standards and Technology (NIST) Standard of Spectral Radiance to the laboratory working standard source, the determination of the white light correction factor, and the testing methods will be presented.

CHAPTER 1

INTRODUCTION

1.1 Multichannel Spectrometers and Array Detectors

The introduction of multichannel detectors has been of significant impact on different branches of spectroscopy. One of the major impacts is on Raman spectroscopy [1]. The array detectors used in multichannel spectrometers opened the door to measure the spectrum of very weak scatterers [1] and the simultaneous detection of spatially dispersed radiation. In general, the combination of multichannel spectrometers and array detectors makes the Raman measurements more sensitive and efficient. The multichannel advantages also extend to an improved abscissa accuracy compared to scanning spectrometers. In addition to the many advantages of multichannel-array detector systems, they have also raised several technical problems [1]. A major disadvantage is that the area of the detector limits the spectral region measured at any given time. This limitation forces the requirement to connect several spectra together in order to obtain the whole Raman spectrum for the analyte of interest. The smoothness of these connections depends on appropriate abscissa and sensitivity

calibrations [1]. Accurate abscissa calibration is critical but there are adequate procedures to perform it on a routine basis [2]. Adequate sensitivity calibration is one of the most challenging problems that remains to be solved.

The sensitivity calibration problem involves both channel-to-channel sensitivity variations and the variations of each channel with wavelength. Several attempts to solve this problem have been made, but present methods are either too tedious to do in routine operations [2,3] or they only correct sensitivity variations within a window. We define a window as the spectral wavelength range measured at one time by the multichannel - array detector system. A calibrated white light source is required to correct both types of sensitivity variations.

1.2 Standard Method to Correct Sensitivity Variations

The current standard method to correct sensitivity variations within a window involves the normalization of the measured white light spectrum as the key step. The procedure is simple. We first record the spectrum of a standard white light source at the best signal-to-noise ratio (S/N) for the given window of interest. The next step is to subtract the dark current spectrum from both the white light spectrum and the sample spectrum for the window of interest. Now, we normalize the white light spectrum by dividing the spectrum by its largest

intensity value. The last step is to divide the sample spectrum by the normalized white light spectrum.

We are making two key assumptions by using this method. First, we are assuming that the sensitivity pattern can be removed by the measurement signal of one which has been made with a light of unit intensity. Second, we are assuming that the white light spectrum intensity is constant across the wavelength range of the detector. There are some problems with the assumptions just mentioned. Among these problems we rapidly realized that the tungsten white light spectrum does not have unit intensity. Furthermore, the white light intensity is not constant over the whole wavelength range of the spectrometer. Even within a given window, we cannot state that the white light intensity is nearly constant, unless we look to a very narrow range. These problems suggest that the assumptions made above will not hold valid for corrections among different windows if we want to compare them. The limitations of this method are as follows. Each window stands alone after sensitivity correction with white light. The intensity ratio of peaks across the whole range under study is not meaningful nor useful when you try to compare different windows. Most importantly, current sensitivity correction with the normalized white light does not allow the use of the white light source as a standard method for monitoring changes in the optical performance of the spectrometer from one working

session to another.

1.3 Development of a New Method for Sensitivity Correction

The method to correct sensitivity variations using a normalized white light works very well within a window. Nevertheless, we must pursue a more effective method if we are attempting to combine several windows to get the complete spectrum of the analyte of interest. Our efforts must strive to develop a suitable and reliable laboratory standard white light source and a sensitivity correction method for multichannel spectrometers. The general concept of our approach is simple. First, we must transfer the calibration of a spectral radiance standard source to a more convenient laboratory working standard source for use on a routine basis. Once this major step is accomplished, then we can use this calibrated laboratory working standard white light source in combination with a fiber optics probe to reproduce the same sampling geometry that will be used in the actual measurement of a Raman spectrum using the same fiber optics probe to image the scattered radiation at the entrance slit of the spectrometer. This arrangement will ensure that we can develop a reliable correction for sensitivity variations both within any given window and interwindows. Such correction method will allow us to connect different spectra smoothly to get the complete Raman spectrum of the sample of interest.

CHAPTER 2

CALIBRATION TRANSFER FROM THE STANDARD OF SPECTRAL RADIANCE TO THE LABORATORY WORKING STANDARD WHITE LIGHT SOURCE

2.1 Introduction

2.1.1 Problem Statement

The use of a calibrated white light source to correct for sensitivity variations in multichannel spectrometers has been well documented in the literature [1,3]. The use of a least-squares-fitted fluorescence spectrum of quinine to perform sensitivity calibration has been discussed in detail by Hamaguchi [1]. These methods are adequate for the sensitivity correction in itself but lack the flexibility and simplicity required for routine operations. For example, we could use the spectral radiance standard developed by the National Bureau of Standard (now National Institute of Standard and Technology, NIST) in 1960 [4], to measure the white light spectrum for the same spectral region of interest in our sample. Then we could develop the appropriate correction factor for our sample spectrum. The problem arises from the inconvenient large size

of this standard of spectral radiance. Both researchers and manufacturers of these standards of spectral radiance agree on how expensive are these sources and that their use should be limited [4]. Therefore it is highly recommended to prepare a working standard that operates at lower current. This working standard should be calibrated against the NIST standard [4].

An additional aspect to consider is the high sensitivity of the multichannel spectrometers to the alignment of the collection optics [1]. This requirement will force us to use a point-like standard white light source placed at the exact optical axis of the spectrometer [1]. The size of the NIST standard makes this geometry control rather inconvenient, especially when the array detector is a charge-coupled device (CCD). The CCD detector is easily saturated by the intense white light from the standard source at distances under 100 centimeters between the source and the entrance slit of the spectrometer without an attenuator in the optical path.

2.1.2 The Proposed Solution

The alternative to the situations previously described is to use a small tungsten filament bulb as the working standard white light source. A source of this type will be compact, easy to handle in any required configuration for the measurements. This small tungsten filament white light bulb could easily be positioned such that the sampling geometry

simulate that used in the actual measurement of the Raman scattering. Fryling et al [3] very accurately described this situation when they stated that the ideal calibration source will :

1. be a weak white light source with a known intensity versus wavelength response curve
2. be placed at the sample position
3. have a size comparable to the Raman scattering area.

2.1.3 The Scope

We will present our approach to transfer the calibration from the NIST standard to a small tungsten filament bulb that will serve as the laboratory working standard white light source. Our approach is simple:

1. Define the sampling geometry for both the NIST standard and the laboratory working standard white light sources.
2. Determine the polynomial equation that defines the spectrum for the NIST standard white light source.
3. Determine the shape of the true spectrum of the laboratory working standard white light source.
4. Determine the polynomial equation that defines the

true spectrum of the laboratory working standard white light source.

2.2 Theoretical Background

2.2.1 Sampling Geometry Control

The calibration transfer procedure requires that we carefully define the sampling geometry that will be used with both white light sources. We designed a white light source holder for the laboratory working standard and one for the NIST standard. The purpose of these white light source holders is to control the geometry of the interface between the fiber optics probe and the white light source. The control over the interface between the white light source and the fiber optics probe will ensure a better reproducibility of intensity measurements (avoidance of ordinate errors) under the same conditions.

The key point for the white light source holder of the NIST standard is to have the minimum number of intervening optics between the source and the collection fiber optics probe. The intensity should be adjusted by the distance between the source and the fiber optics probe to avoid oversaturation of the CCD detector. The intensity of the source could also be reduced by means of an attenuator, but the transmittance of the attenuator must be exactly known if absolute intensity measurements are to be carried out. The

size of the white light source holder for the NIST standard should not be a major concern as long as it is feasible. Two major requirements exist for this white light source holder. The fiber optics probe must be exactly aligned in the optical axis of the light beam coming from the tungsten ribbon of the source. The reason for this requirement is to ensure that the light collected by the fiber optics probe is mainly the light passing through the fused-silica window. The radiation passing through the fused-silica window is coming from the center of the tungsten ribbon which has been calibrated against a blackbody source and the irradiance is constant [5]. The second requirement is that the white light source radiation illuminate the fiber optics probe uniformly.

The white light source holder for the laboratory working standard should be compact, easy to handle, and provide uniform illumination of the fiber optics probe. Attenuators such as neutral density filters may be employed as long as reproducibility of these elements is possible. We do not have to impose hard demands on the characterization of the attenuators used in this arrangement because the calibration transfer will be carried out by comparing the laboratory working standard source of radiation with the NIST standard. Under these conditions we are treating the white light source, the holder-defined sampling geometry, and the fiber optics probe as one large system that represents a specific source to

be imaged at the entrance slit of the spectrometer [3,4]. Therefore, no knowledge of the specific characteristics of the attenuators or the source holder for the laboratory working standard in itself is required as long as the same fiber optics probe and collection external optics are used to image the source radiation at the spectrometer slit.

2.2.2 Spectral Radiance Sources

Since 1910, a great need for a convenient standard of spectral radiance has driven the search for a secondary standard source for practical applications in spectroscopy. The blackbody was then and today the absolute reference standard, but it is only of practical use for very specialized laboratories [4]. Stairs et al published in 1960 a very informative paper on the new secondary standard of spectral radiance for the region of 250 nanometers to 2,600 nanometers. This new secondary standard was a tungsten strip lamp designed at the National Bureau of Standard and calibrated against a blackbody.

The blackbody radiation characteristics, both total and spectral can be described by **Planck's radiation law**. In simple terms, the spectral radiance of a blackbody at any particular wavelength B_{λ}^b can be directly related to the absolute temperature T by the following alternative form of Planck's law [4,6]:

$$B_{\lambda}^b = C_1 \lambda^{-5} / e^{C_2 / \lambda T} - 1 \quad (2.1)$$

where $C_1 = 2hc^2 = 1.19088 \times 10^{16} \text{ W nm}^2 \text{ cm}^{-2} \text{ sr}^{-1}$ is the first radiation constant and the second radiation constant is defined as $C_2 = hc/k = 1.438 \times 10^4 \text{ nm K}$. Once this relation is recognized, then a blackbody can be easily used as a reference for the development of the new secondary standard of spectral radiance.

The research on tungsten lamps demonstrated that under well controlled conditions the emissivity of a pure clean tungsten ribbon is constant throughout the life of the lamp. The spectral distribution of spectral radiation from the tungsten lamp cannot be calculated from the emissivity values published in the literature [4]. The problem arises from many factors such as impurities in the filament as well as its size and shape. Even interreflections within the lamp envelope can affect the total spectral radiation measured. These are the reasons for the calibration of the tungsten lamp against a blackbody.

The standard of spectral radiance uses a flat-ribbon of tungsten in order to avoid the effects of the angle from which it is viewed. This precaution will ensure a reproducible source [4]. The radiant energy of this flat-strip passes through a 3 cm diameter fused-silica window [5] located

parallel at a distance of 3 to 4 inches from the center of the flat-strip of tungsten [4]. This design serves a very practical use of reducing the deposit of metallic tungsten on the surface of the fused-silica as the lamp ages. During calibration of the tungsten lamp against the blackbody, the glass envelope is in vertical position to allow the collection

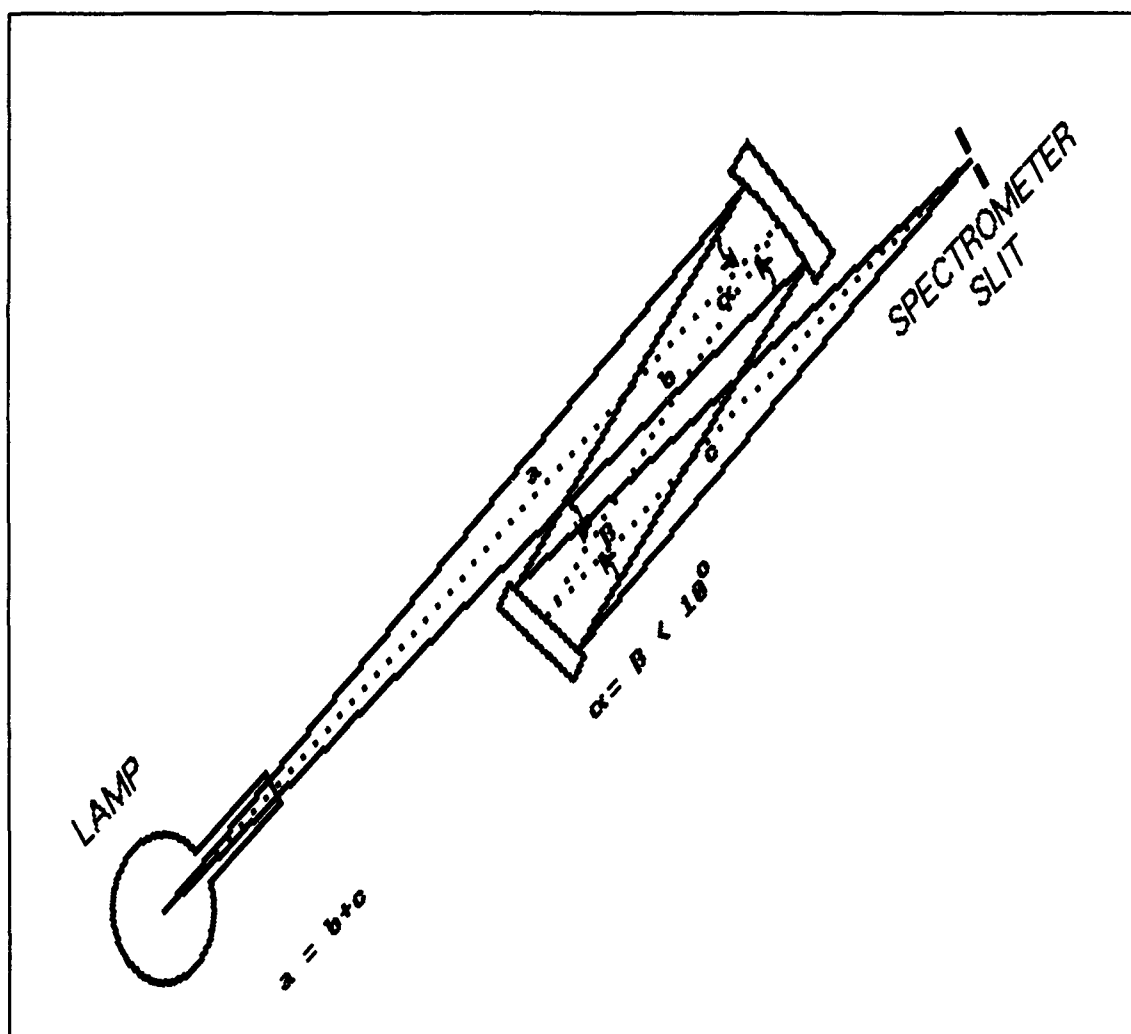


Figure 2.1: Arrangement of External Optics to Focus the Image of the Tungsten Filament at the Entrance of the Radiometer[5]

optics to achieve a horizontal view through the center of the fused-silica window. External optics collect and focus a full size image of the central section of the tungsten ribbon at the entrance slit of the radiometer; see Figure 2.1. Therefore there is no need to measure the exact area of the tungsten flat-strip, because the entrance slit of the radiometer will determine the source area used in the measurements [4,5].

Several precautions were taken during the calibration of the tungsten lamp against a blackbody in order to minimize sources of errors or uncertainties. First, the readings were alternately taken on the blackbody and the tungsten lamp [4] for each wavelength setting of the spectral range of interest. The cone of radiant energy collected from the lamp was 5 degrees in the original calibration method [4], but most recent calibration procedures [5] used a smaller angle of only 2.5 degrees. It is important to realize how the calibration of these lamps is done against a blackbody because any application that requires a larger cone of radiant energy must also involve a way to ensure that the irradiance is constant over the whole aperture. Our experimental arrangement ensures the collection of a cone angle within the limits just discussed. Section 2.2.4 discuss details about solid angle collected and section 2.3.2 discuss the actual sampling geometry defined by the source holders. Excessive water vapor in the laboratory atmosphere may absorb at certain wavelengths

introducing errors in the calibration [4]. These effects are very significant in the infrared region but not so important in our wavelengths region of interest. Nevertheless, the calibration method cancels out most of these water vapor absorption effects by measuring both the blackbody and tungsten lamp with identical air path [4].

The use of the standard has been discussed in detail elsewhere [4,5], but some important points will follow. First, it is highly recommended that a full size image of the central section of the flat-strip of tungsten be focused at the entrance of the spectrometer when using this source to calibrate it. Second; experiments that involves the comparison of two sources of radiation do not require knowledge of the spectral reflectance of collection optics, of the spectrometer transmission characteristics, or the spectral sensitivity of the detector. If the same collection optics are used for both sources, there is no need for the measurement of the dimensions of the spectrometer slit as long as the slit is fully and uniformly filled by both sources. Third; these sources should be operated on alternating current to avoid filament crystallization effects caused by direct current. These lamps require a very stable power supply in order to reduce fluctuations in the operating current at which the lamp has been calibrated. Fourth, the standard is very expensive source, \$2,400 each, and very fragile. It is highly

recommended to limit their use to calibrate other working standards that operate at lower currents.

The requirements for a reliable laboratory working standard white light source are of great importance on its selection. The laboratory standard must be able to maintain its initial level of light output for a long period of time, such as weeks or months. Furthermore, once this output level is not maintained within useful limits, then its desirable that the white light bulb undergo total failure instead of a slow decay with time. We selected the Welch-Allyn tungsten-halogen lamp for its high output at a given wattage and excellent maintenance of initial output.

2.2.3 Fiber - Optic Probes

Fiber-optic probes offer outstanding advantages for Raman scattering measurements as discussed by C.K. Chong et al [7]. Many of these advantages translate directly to the experimental control of the calibration transfer from the NIST standard to a laboratory working standard white light source. The following discussion briefly describe some of the characteristics of the bifurcated fiber-optic probes used in this research and how they simplify the experimental control of the measurements.

Fiber-optic probes, in general, are mechanically

flexible, which allows radiant energy to be transmitted over curved paths without problems. Certainly, fiber-optic probes simplify the type and number of auxiliary optical components required to transmit radiant energy between any two given point of the optical system in place. Fiber-optic bundles contain a known number of fibers with a very small diameter. Multifiber systems, such as the bifurcated fiber-optic bundle, can conduct laser radiation to the sample with one excitation fiber while using another or several other fibers to collect the scattered radiation from the sample. This feature offers great advantages for Raman experiments in terms of the flexibility of the sampling geometry. Nevertheless, the optical efficiency that can be attained by the fiber-optic probe is mainly dictated by the spectrometer. The spectrometer imposes optical constraints that limit the choices of fiber size and numerical aperture; two of the most important parameters that control the efficiency of the fiber-optic probe. For example, it is only possible to achieve optimum optical matching of the fiber optic-probe and the spectrometer when the ratio of the core diameter to f-number of the fiber matches the ratio of the slit width to the f-number of the spectrometer [7]. A typical arrangement is shown in Figure 2.2, where S_1 is the fiber-to-lens distance, S_2 is the lens-to-slit distance, θ is the exit angle of the fiber-optic probe, and d_L is the limiting diameter defined by the optical lenses employed. The cone of light projected by the fiber-optic probe

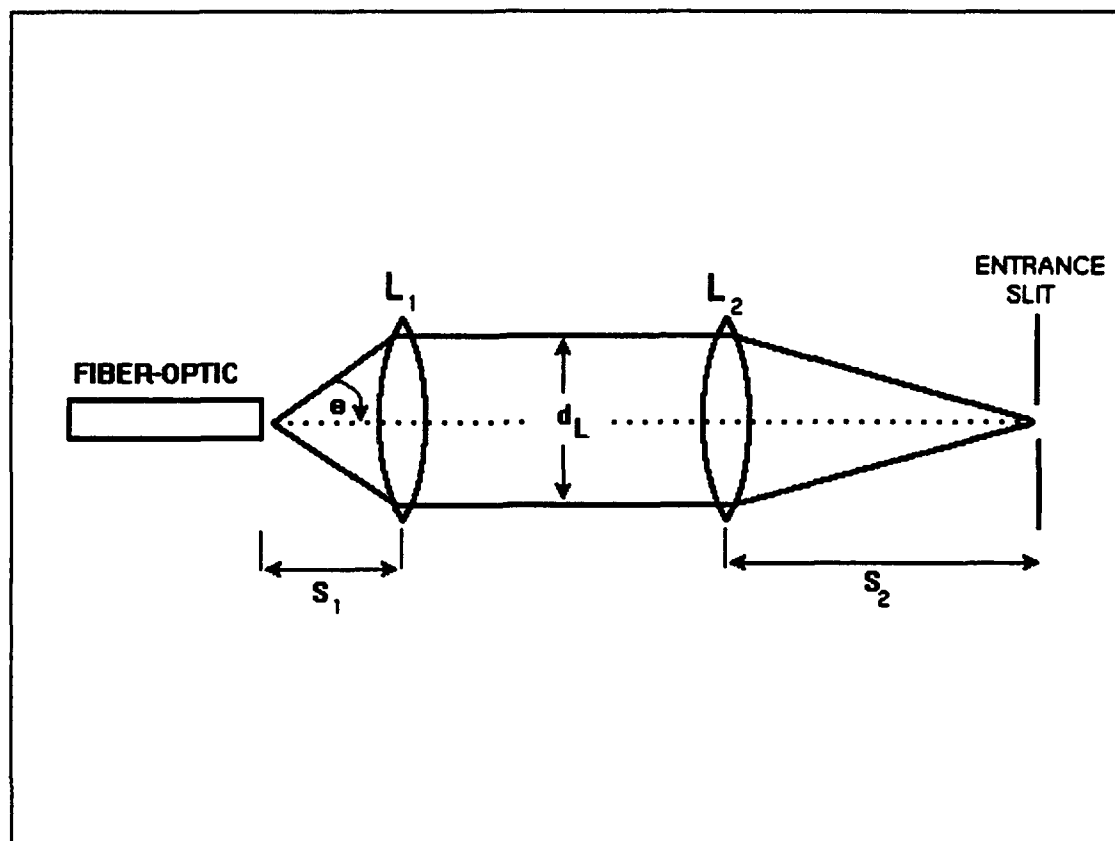


Figure 2.2: Important Parameters to Match the Fiber-Optic Probe With the Spectrometer.

defines the important parameter known as numerical aperture (NA) of the fiber. The expression used to calculate the NA is $\eta_0 \sin \theta$, where η_0 is the refractive index of the medium in contact with the fiber-optic probe. For our purposes, the medium in contact with the fiber is air, therefore $\eta_0 = 1.00$. A second parameter of great importance, the f-number of the fiber-optic probe, is also defined in relation to the arrangement shown in Figure 2.2. The fiber's f-number can be defined as $f/n = (2 \tan \theta)^{-1}$ or simply by the equivalent

expression $f/n = S_1/d_L$. Furthermore, if the ratio of S_2/d_L equals the f-number of the spectrometer, then we can angle-match the fiber-optic to the spectrometer. This action implies that the magnification factor of the image, $M_{\text{img}} = S_2/S_1$, must also equal the ratio of the spectrometer's f-number to the fiber-optic probe's f-number. In general terms, all we are doing is magnifying the image from the fiber-optic probe by the ratio of the f-numbers of the spectrometer and the fiber-optic probe. The purpose is to have the magnified image to just fill the spectrometer entrance slit width as shown in Figure 2.3.

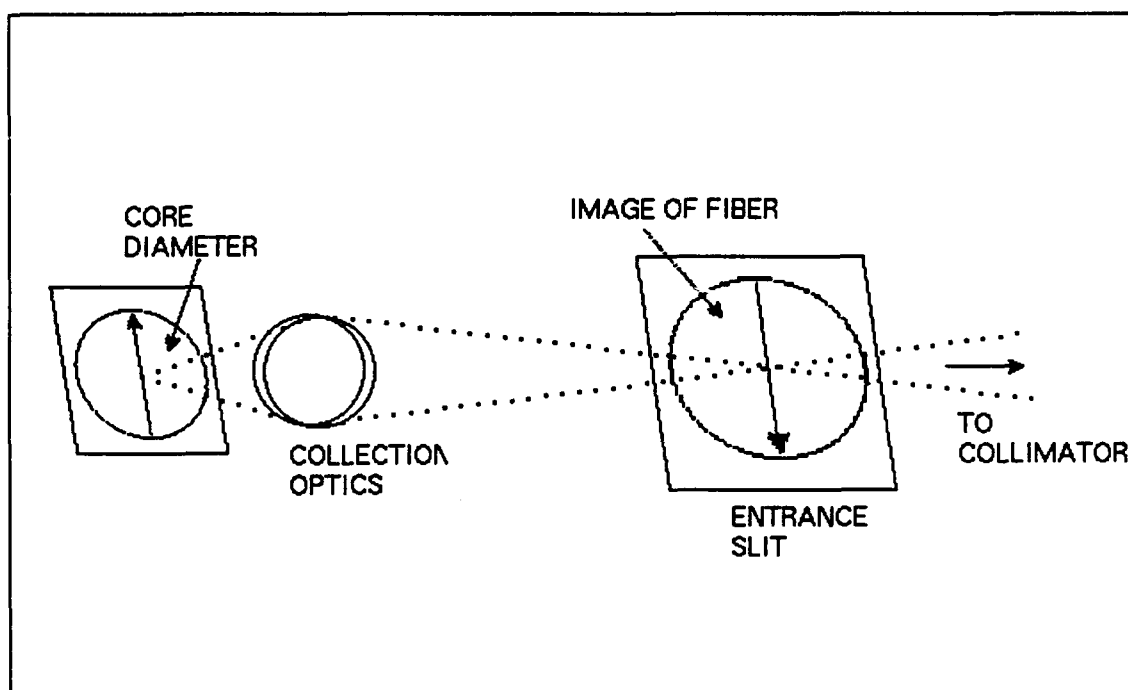


Figure 2.3: Filling the Entrance Slit of the Spectrometer with the Magnified Image.

Once the optimum optical matching is achieved, the next consideration is the collection efficiency of the particular multi-fiber arrangement. We use two systems in our research that employ all fibers of the same size and in a close-packed configuration with their faces positioned in the same plane. The first system consist of two fibers, one excitation fiber and one collection fiber. The second system consists of seven fibers, one excitation and six collection fibers (1X6 system). The 1X6 system has the six collection fibers surrounding the excitation fiber at the sample end [7]. At the spectrometer's end, these collection fibers are arranged in a 1X6 configuration with the long axis parallel to the slit height of the spectrometer entrance slit [7]. Figure 2.4 shows the

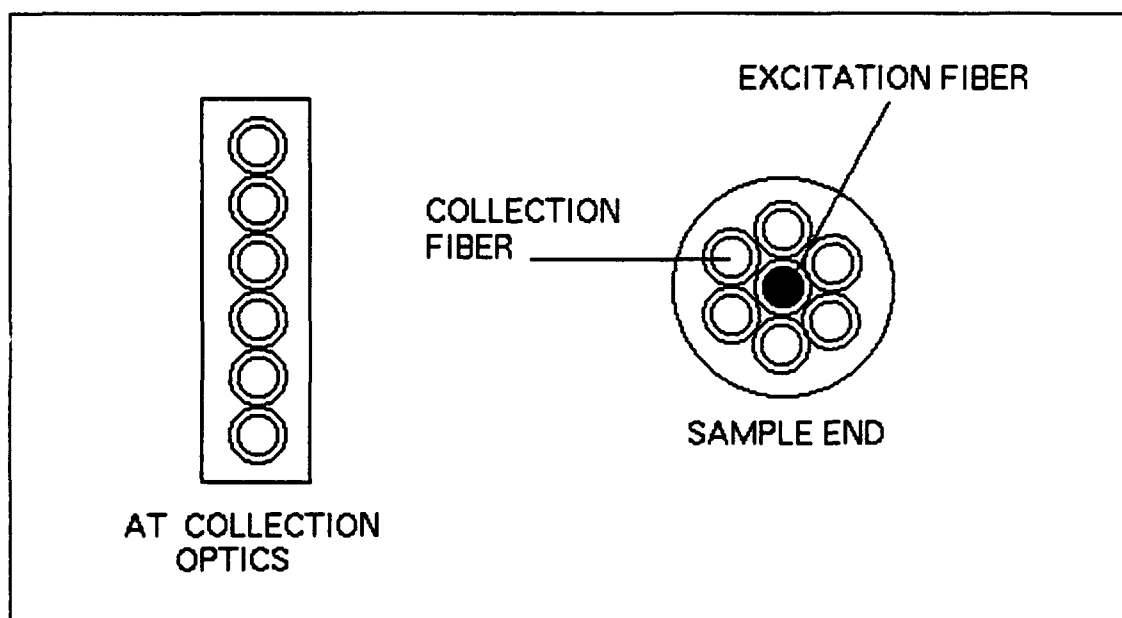


Figure 2.4: 1X6 Configuration of Fiber-Optic Probe.

display of the 1X6 fiber just described. The two-fiber system (1X1) has a well defined overlapping area between the excitation and collection cones at a fixed distance from the plane containing the faces of the two fibers [7]. Figure 2.5 shows a description of the overlapping area for this fiber-optic system; where r_{fo} is the radius of the fiber-optic, r_c is the fiber core radius, and d is the minimum distance between the fiber cores. There is an optimum distance for maximum overlap of the excitation and collection cones; any distances below this fixed value will significantly reduce the degree of

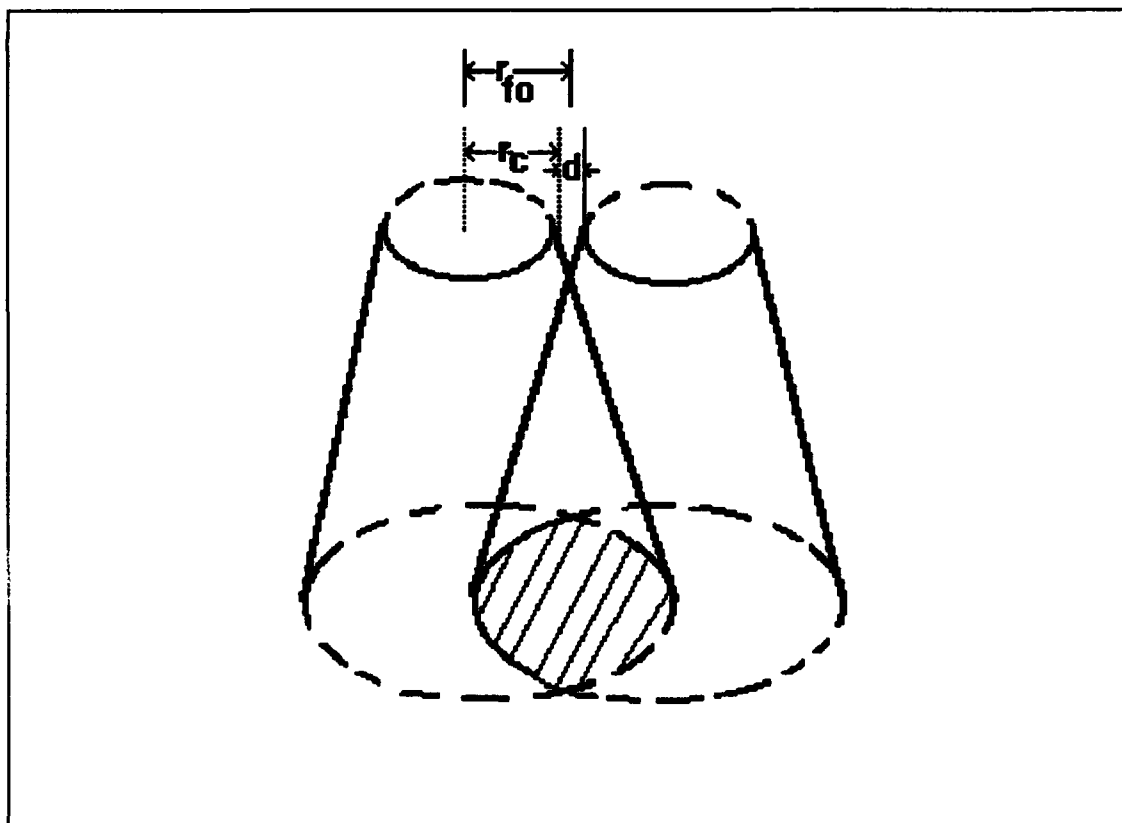


Figure 2.5: Overlapping Cones Area of 1X1 Fiber-Optic Probe.

overlap and the collection efficiency. The importance of the collection efficiency and of its detailed definition becomes critical when the fiber-optic probe will be used to collect the radiant energy from the sources of white light employed for the calibration transfer. It is to our advantage, although not required, that the fiber-optic probes configuration employed for normal Raman measurements can also be used to collect the radiation energy of the white light sources during the calibration transfer from the NIST standard and the laboratory working standard white light source. The reason behind this statement is that we must characterize the response of the fiber-optic probe with the output of a calibrated white light source in order to mimic the actual sampling conditions of a Raman measurement. The fiber-optic probe will become a secondary standard that has characteristics similar to that of a Raman scatterer of known specific intensity [3]. The fiber-optic probe has the capability to collect radiant energy from a calibrated standard white light source of known intensity and convert it into a specific intensity standard [3] that can easily be interfaced with the external optics of the spectrometer, as shown in Figure 2.2. It is important to recall at this point the many constraints imposed in the optical arrangement when using the NIST standard in order to prevent distortion of the image of the central part of the tungsten filament that must be projected at the entrance slit of the spectrometer [4,5];

see Figure 2.1. Some of these constraints or precautions are the use of precise optical surfaces and the requirement to keep the angles between incident and reflected beams to less than 10 degrees [4,5]. The use of the appropriate fiber-optic probe, given the constraints imposed by the spectrometer in size and numerical aperture, satisfies all these requirements to avoid distortion of the filament image and loss of radiant energy.

Transmission losses due to bending and coiling of the fiber-optic probe is another factor that must be controlled and well defined. Myrick et al [8] reviewed in detail these bending losses of fiber-optic probes. There are some important parameters that must be observed in order to minimize the transmission losses due to bending and coiling of the fiber-optic probes in the experimental set up of convenience. First, parallel fiber configurations or bundles, due to their small size do not show significant losses unless you are required to have dual fibers at 90 degrees to one another. Second, significant losses will occur when the radius of curvature is reduced to 7 mm or less. Myrick et al demonstrated [8] that transmission losses will occur not only as a function of the radius of curvature, but also as a function of the number of turns in the fiber. The greater losses occur in the first turn of 360 degrees. A third point is that good excitation throughput is not necessarily an indication of good collection

throughput, especially if bends and kinks of the fiber are uncorrected. We can see that many of the losses in transmission efficiency of the fiber-optic probe can be avoided or controlled. The important point is that we must be aware of these possible losses and when they cannot be avoided, then the efforts must be put into making them reproducible from one measurement to the next while performing the calibration transfer between the NIST standard and the selected laboratory working standard white light.

2.2.4 Definition of Theoretical Parameters:

The first parameter we must characterize within the defined geometry is the radiant output of the fiber optic probe in combination with the source of spectral radiance or white light, F_{λ} :

$$F_{\lambda w} = B_{\lambda} T_{att} \Omega_{fib} T_{fib} \quad (2.2)$$

The $F_{\lambda w}$ is expressed in units of watts $\text{cm}^{-2} \text{nm}^{-1}$. The spectral radiance output, B_{λ} , is expressed in units of watts $\text{nm}^{-1} \text{cm}^{-2} \text{sr}^{-1}$; the transmittance of the attenuator T_{att} , is unitless; T_{fib} is the transmittance of the fiber-optic probe; and Ω_{fib} is the solid angle collected by the fiber-optic probe. We define the solid angle collected by the fiber optic probe as the ratio of the area of the fiber optic probe, A_{fib} , to the square of the distance from the fiber optic to the source, d^2 :

$$\Omega_{fib} = A_{fib} d^{-2} \quad (2.3)$$

where

$$A_{fib} = (\pi/4) D^2 \quad (2.4)$$

and D is the diameter of the fiber optic probe.

The radiant output of the fiber-optic probe with white light source can also be expressed in terms of units of photons $s^{-1} nm^{-1}$ in the following manner:

$$F_{\lambda p} = (B_{\lambda} \lambda / hc) A_{fil} T_{im} \Omega_{fib} T_{fib} \quad (2.5)$$

where $hc = 1.986 \times 10^{-16} J nm$, and A_{fil} is the area of the filament that is projected at the entrance slit of the spectrometer.

$$A_{fil} = (w_{slit} \times D_{fib}) / M_{img} \quad (2.6)$$

The area of the filament is defined by the intersection of the spectrometer's entrance slit width, w_{slit} , and the diameter of the fiber-optic probe, D_{fib} . The image's magnification factor, M_{img} , is given by the ratio of distance from the focusing lens to entrance slit, to the distance from the fiber-optic probe output end to the focusing lens, $M_{img} = S_2/S_1$.

The magnified image is shown in Figure 2.6. Both the width and the height of the filament's image are magnified as shown in Figure 2.7. There are several points of interest on these relations between the magnified filament's image, the area of the image collected by the spectrometer and the actual area of the filament's image collected by the fiber-optic

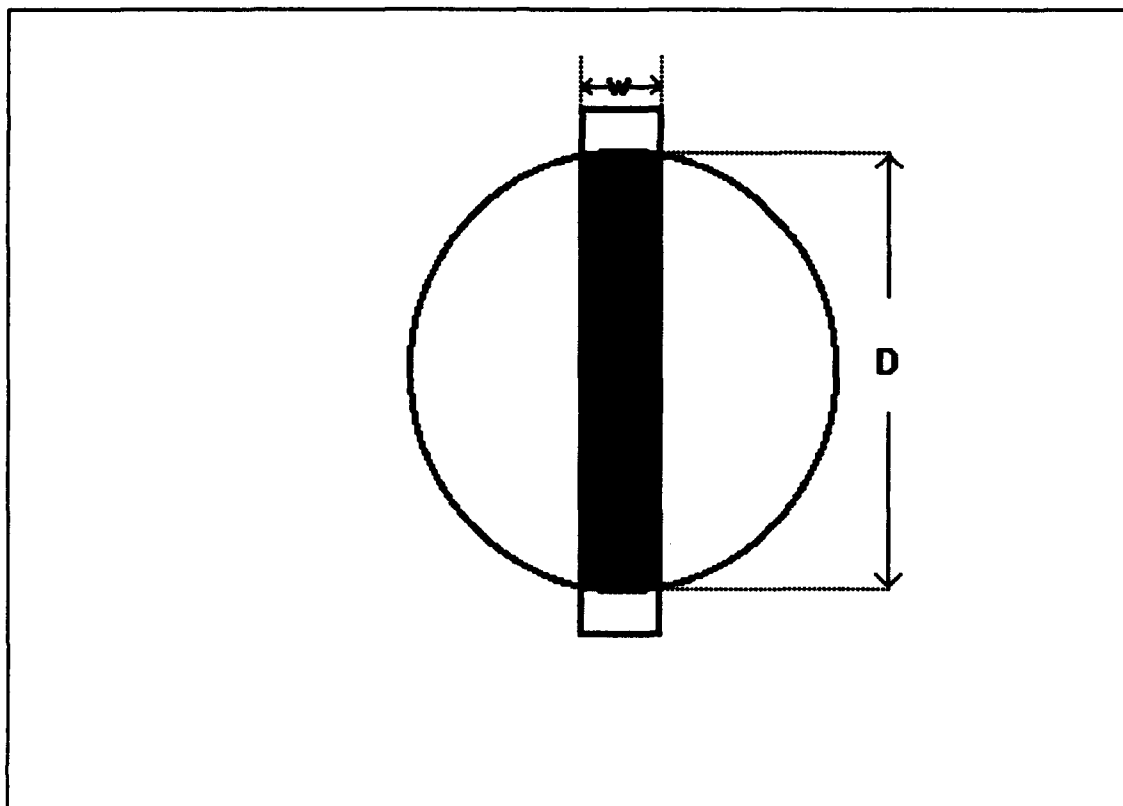


Figure 2.6: Area of the Filament Defined by the Magnified Image and the Spectrometer's Slit.

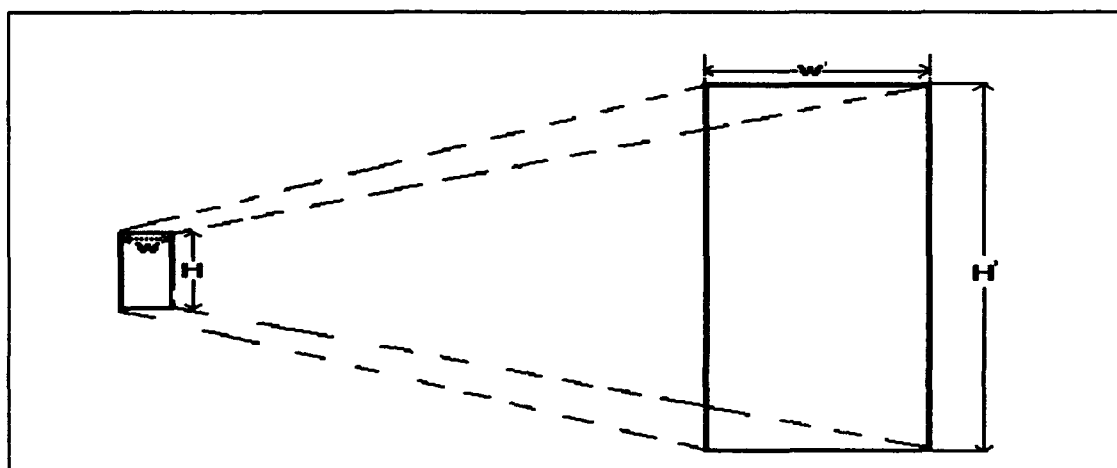


Figure 2.7: Magnification of the Filament Image's Width and Height.

probe. Both the width and height of the filament's image are magnified by a fixed factor for the optical system in use. In order to get the dimensions of the actual filament's image collected by the fiber-optic probe, we must consider only a fraction, $1/M_{\text{mag}}$, of the image projected at the entrance slit. There are two implications from this statement. First, the slit height of the spectrometer is very large compared to the diameter, then it is the diameter of the projected image that determines the height of the image collected by the spectrometer. The diameter of the image from the fiber-optic was magnified by the same factor M_{mag} that we must divide by in order to get the actual height of the filament's image collected. Therefore, we can simply state that the diameter of the fiber-optic probe used to collect the image of the filament defines the actual height of the filament in the collected image. Second, the width of the filament's image is also magnified, but unlike the height of the collected image, the width is determined by the slit width of the entrance slit of the spectrometer. The reason for this approach is that we are taking a fixed fraction out of the filament's magnified image defined by the slit width. Therefore, in order to obtain the width of the actual filament's image collected by the spectrometer, we must divide the slit width by the magnification factor.

2.3 EXPERIMENTAL

2.3.1 Calibration Transfer General Steps.

The description of the calibration transfer can be summarized in five main steps. The first step is to determine the equation that describes the behavior of the shelf standard white light source. We used a Standard of Spectral Radiance from the National Institute of Standard and Technology (NIST) as the shelf standard white light source. The manufacturer provides information of the spectral radiance in watts $\text{nm}^{-1}\text{cm}^{-2}$ versus wavelength, in nanometers, for a range of interest. A simple plot of these data will afford the working material to determine the order of the polynomial equation describing the behavior of the source in the wavelength range of interest. We can fit a spline to determine the order and the coefficients of the polynomial equation of the shelf standard white light source.

The second step in the calibration transfer is to measure the experimental relative intensity counts for both white light sources, the shelf standard and the laboratory working standard. Measurement of the output of these sources should be under similar conditions. The information collected from these measurements will be used to calculate the average intensity for the central wavelength of each window in the range of interest. We define a window as the actual physical wavelength range that can be simultaneously covered by the array

detector. The intensity at the central wavelength of each window for each white light source will provide us a more reliable measurement of the intensity trends of each source.

The third step on the calibration transfer involves the calculation of the ratio of the intensity counts of the laboratory working standard to the intensity counts of the shelf standard source $R_{L/S}$; for each window. The ratio of intensities of both sources give us the opportunity to eliminate the effects of instrumental and sampling geometry features in common for both sources. Let us consider the intensity counts of white light at any given pixel P , called S_{FP} :

$$S_{FP} = F_{\lambda P} T_{OPT} T_{SLT} T_{SPG} Q_{DET} D_{n/p} W_{pix} G t \quad (2.7)$$

where $F_{\lambda P}$ is the radiant output of the white light source in photons/s nm. T_{OPT} is the transmittance of the optics in use. T_{SLT} is the transmittance of the spectrometer entrance slit given by the ratio of the area passed by the slit to the image area. T_{SPG} is the transmittance of the spectrograph, due to the grating efficiency, reflection losses, and other instrumental factors that all together generate a specific dependence of this parameter on wavelength and pixel position. Q_{DET} is the quantum efficiency of pixel P , in electrons per photon. $D_{n/p}$ and W_{pix} are the dispersion in nanometers per pixel and the

width of a pixel respectively; the product of these two parameters will determine the bandpass if we assume that the pixel width is less than the slit width. Finally, G is the gain of the amplifier and analog-to-digital (A/D) converter, in counts per electron; and t represents the integration time in seconds, used in the measurements. All these parameters, except $F_{\lambda p}$, can be accounted for and basically eliminate their contributions to the intensity counts at any given pixel just by taking the ratio described above. This approach will work effectively as long as a good pixel registration is achieved between both white light sources.

The fourth step of the calibration transfer involves the determination of the output of the laboratory working standard white light source with the fiber-optic probe, $F_{\lambda w}$, in watts $\text{nm}^{-1} \text{cm}^{-2}$. This calculation is simply carried out by multiplying the ratio of intensities of the laboratory working standard source to the shelf standard source, $R_{L/S}$, by the radiant output of the shelf standard white light source.

$$\text{LAB } F_{\lambda w} = (R_{L/S}) (\text{SHELF } F_{\lambda w}) \quad (2.8)$$

Following this operation, we can carry out the fifth and last step of the calibration transfer: determination of the $\text{LAB } F_{\lambda p}$ and the equation describing the behavior of the laboratory working standard white light for the wavelength

range of interest. Fitting a spline to the plot of **LAB $F_{\lambda p}$** versus the central wavelength of each spectral window will determine the order and coefficients of the polynomial describing the curve.

2.3.2 Instrumentation

The dispersive Raman system used in this research consists of a Jobin-Yvon HR640 spectrograph of 640 mm focal length and a 1800 grooves/mm holographic grating blazed at 500

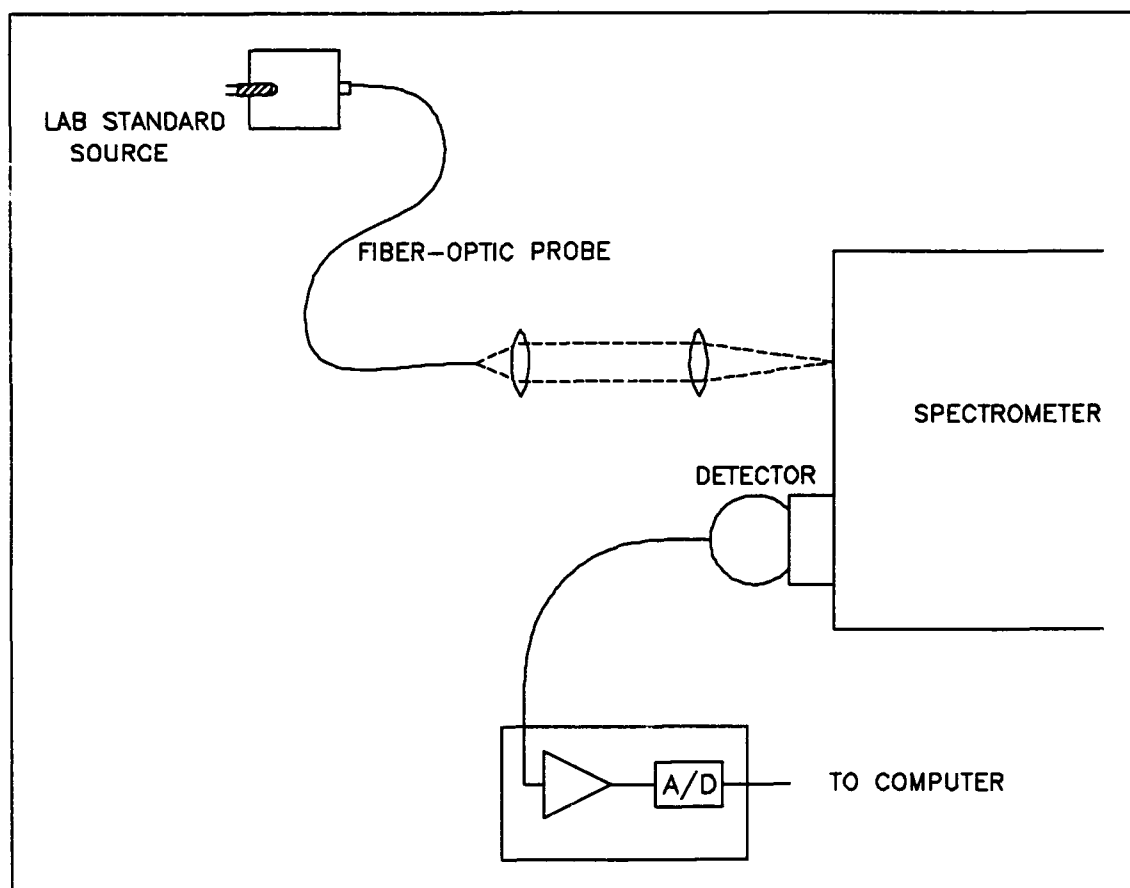


Figure 2.8: Dispersive-Raman System with Fiber-Optic Probe and CCD Detector.

nm providing a dispersion of 0.8 nm mm^{-1} with an aperture of $f/5.7$. A general scheme of the system used is shown in Figure 2.8. Two liquid nitrogen cooled charge-coupled devices (CCD) from Princeton Instruments were used for detection. One is an 1152×298 pixel front-illuminated CCD detector and the other is a 1024×1024 back-illuminated CCD detector. We binned 200 to 300 rows in each case. A Coherent Innova 70 argon ion laser was used to generate a 514.5 nm excitation line for the optical alignment checks of the system. Two types of $f/2$ bifurcated fiber-optic probes were employed for the alignment checks as well as for measurements of spectral radiation from white light sources. The 1×6 fiber optic probe consists of one excitation fiber surrounded by six concentric collection fibers as shown in Figure 2.4. Each fiber has a core diameter of $200 \text{ }\mu\text{m}$. The 1×1 fiber optic-probe consists of two $400 \text{ }\mu\text{m}$,

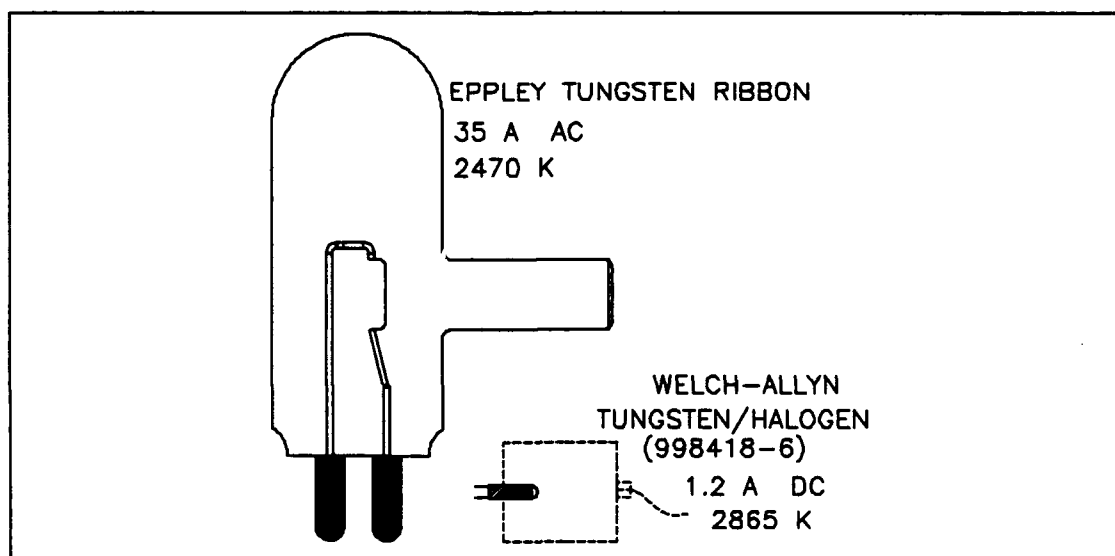


Figure 2.9: Schematic of the Shelf and Laboratory Working Standard White light Sources.

core diameter, parallel fibers, one for excitation and one for collection of radiation. Figure 2.5 shows the 1x1 fiber-optic probe arrangement. Section 2.2.3 of this paper provides more detailed information on the fiber-optic probes employed.

Two white light sources were employed on this research; a laboratory working standard source and a shelf standard source. The laboratory working standard source is a Welch-Allyn tungsten/halogen 1.2 amperes-dc small bulb, model 998418-6, that burns at a constant temperature of 2865 K. The shelf standard employed is the "NBS Standard of Spectral Radiance" G.E. 30A/T24/17 model (Serial No. EPT-1109) from The Eppley Laboratory, INC. The Standard of Spectral Radiance is a tungsten ribbon lamp with a working current of 35 amperes-ac and a temperature of 2470K. This shelf standard was calibrated at 35 wavelengths, from 250 nm to 2600 nm, against NIST's reference standards. Figure 2.9 shows a schematic diagram of both sources. A detailed discussion of the characteristics of these sources can be found in section 2.2.2 of this paper.

Locally designed holders were used to define a reproducible sampling geometry for each white light source. The laboratory working standard white light source holder is shown in Figure 2.10. This holder has a slot for the exact and fixed positioning of the laboratory standard source. The light from the source can be attenuated by a neutral density filter

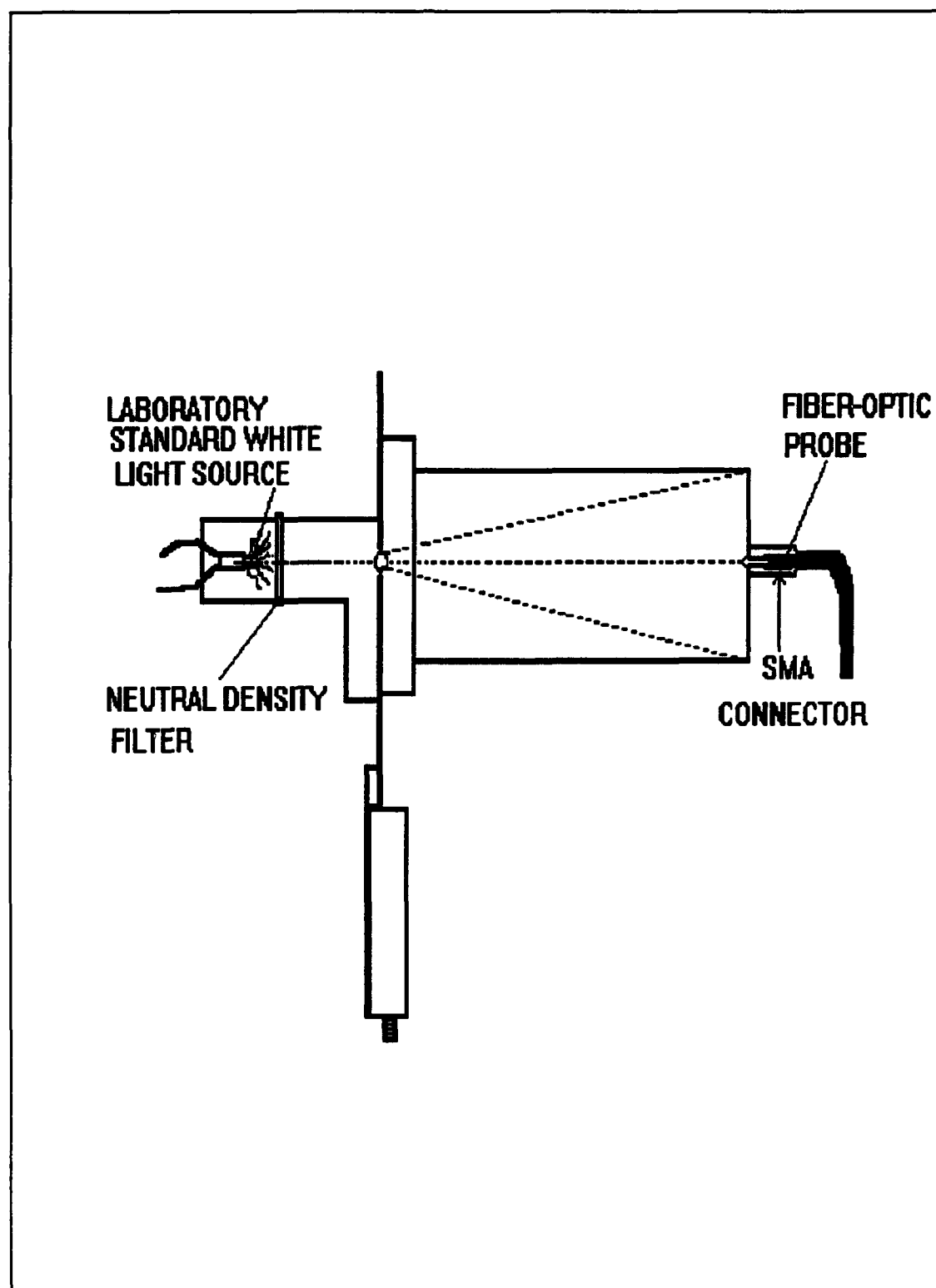


Figure 2.10: Current Laboratory Working Standard White Light Source Holder.

positioned 2.0 cm from the source if required. The metal plate at the main frame provides the limiting aperture to the radiance light reaching the extended tube where the fiber-optic probe is connected. A diffuser is employed between the main frame metal plate and the entrance of the extended tube of the connection port for the fiber-optic probe. The fiber-optic probe is located at a distance of 6.5 cm from the laboratory working standard white light source.

The two versions of the source holder for the Standard of Spectral Radiance are shown in Figures 2.11 and 2.12. The

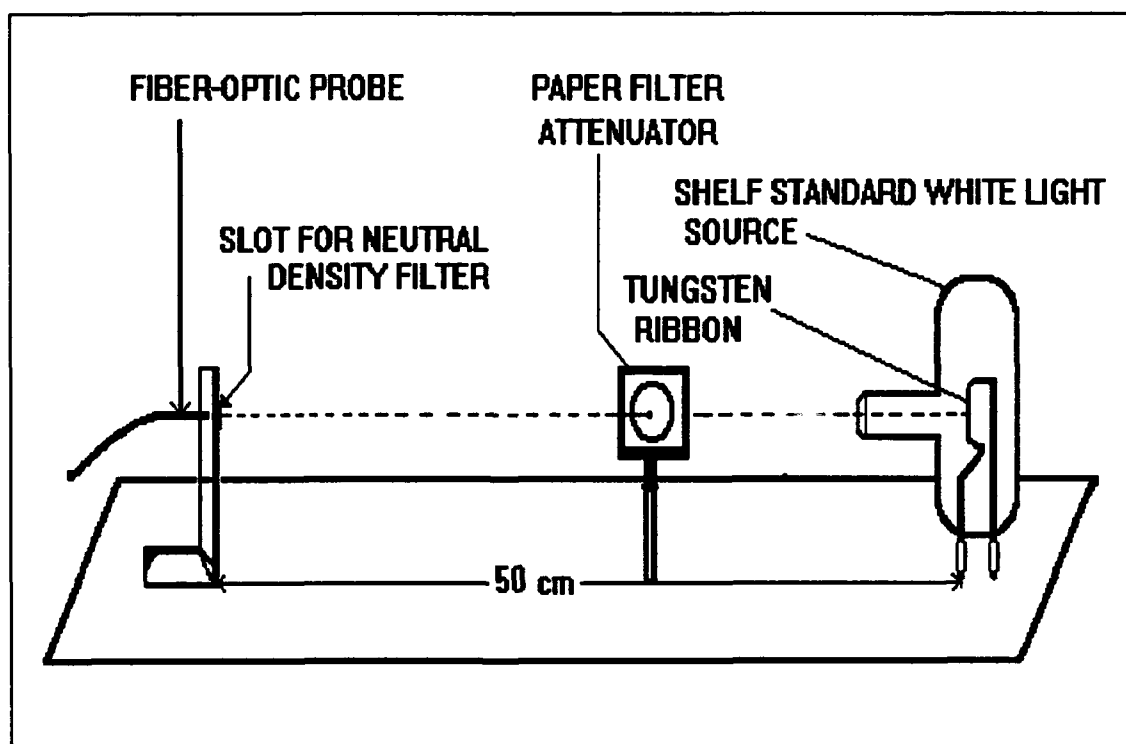


Figure 2.11: Shelf Standard White Light Source Holder 1.

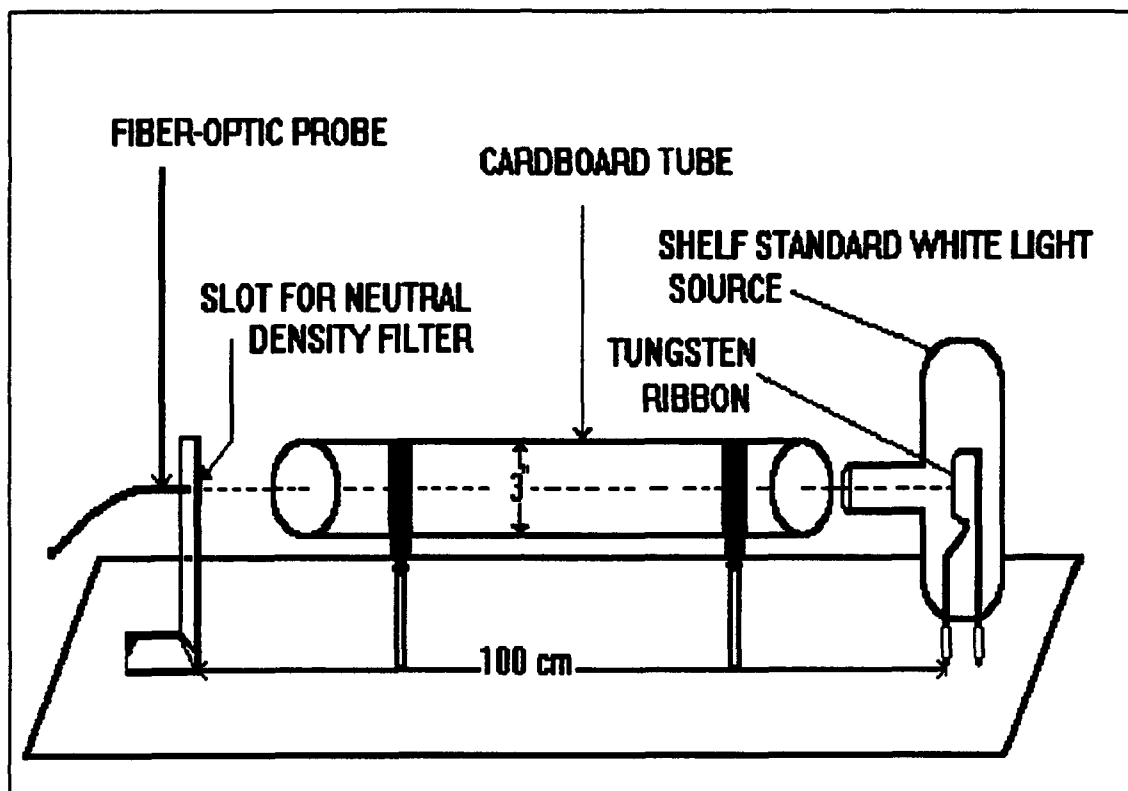


Figure 2.12: Shelf Standard White Light Source Holder 2.

Standard of Spectral Radiance is securely affixed to a mount screwed in a metal plate that serves as the base for the support of the holder. A metal plate screwed to the metal base plate serves as the connection port for the fiber-optic probe and also provides a slot for a neutral density filter just in front of the fiber-optic probe. The fiber-optic probe is located at 50 cm, for the first model and at 100 cm from the tungsten ribbon in the source, in the second model. Both models have the fiber-optic probe carefully aligned with the center of the flat tungsten ribbon. A black cardboard tube, 3 inches in diameter, is located between the source and the

collection point of spectral radiation to prevent light rays not generated at the center of the ribbon to reach the fiber-optic probe.

2.3.3 Measurements

We used the same measurement conditions for the spectra of both white light sources. CCD detectors were cooled down to -110°C to minimize the effects of dark current. The spectrometer slit width was set to $300\text{ }\mu\text{m}$, the typical value expected for a Raman measurement. A total of 100 s integration time was used for each spectrum; 100 repetitions of 1 s exposure coadded. The fiber-optic probes used in our system insure that the white light sources images are properly aligned with the entrance slit of the spectrometer. According to the external collection optics of the spectrometer, the effective source of spectral radiance is the end of the fiber-optic probe illuminating the entrance slit. Both white light sources are interchanged by moving the collection end of the fiber-optic probe from one source to the other. The idea is to make both white light sources to occupy the same space at different times with respect to the spectrometer as long as the fiber-optic probe is uniformly illuminated. Our wavelength of interest extend from 490 nm to 675 nm. We divided this range in 12 spectral windows of approximately 15 nm each, with some overlapping between adjacent windows.

The measurements of the irradiance of both sources can be carried out in two distinctive ways. The first method consists of selecting one of the white light sources to measure the spectra of all twelve windows without moving the fiber-optic probe from the connecting slot. Once the spectra for all twelve windows for the first source have been recorded, then switch the fiber-optic probe to the second white light source holder and repeat the same procedure. The second method is more realistic in terms of Raman measurement conditions. This second method involves switching the fiber-optic probe between white light sources for each window, before moving to the next. We recorded the dark current spectra for each source on each window just prior to the white light spectra measured.

We allowed a warming time to each white light source in order to achieve a stable current and operating temperature of these sources. This is a critical precaution to ensure reliable uniform and constant radiance output of the source. The NIST standard was allowed to stabilize for two hours at a constant operating current of 35 amperes. The laboratory working standard white light source stabilized in 30 minutes at a constant current of 1.2 A.

2.4 Results and Discussion

2.4.1 Polynomial Equation for the Shelf Standard Source

The purpose of this calculation is to establish the

baseline information that we will need in the eventual determination of the true spectrum of the laboratory working standard white light source. The true spectrum of the NIST standard is well known. The manufacturer of the NIST standard provided detailed calibration information on the spectral radiance versus wavelength for the range of 400 nm to 1200 nm. We used this calibration information with the spectral radiance given in $\text{watts sr}^{-1} \text{ nm}^{-1} \text{ cm}^{-2}$, to calculate the theoretical output of the shelf standard white light source combined with a fiber-optic probe, in $\text{watts nm}^{-1} \text{ cm}^{-2}$. Table 2.1 shows the manufacturer's information and the calculated theoretical output of the shelf standard. A plot of this information is shown in Figure 2.13. We fitted several splines

Table 2.1: Theoretical Output of EPT1109 Standard of Spectral Radiance and Fiber-Optic Probe (1x1) at 100 cm Separation.

WVL	B_λ	$F_{\lambda W}$
400	0.000537	1.07E-11
450	0.00131	2.61E-11
500	0.0026	5.18E-11
550	0.00433	8.62E-11
600	0.00631	1.26E-10
650	0.00834	1.66E-10
700	0.0103	2.05E-10
750	0.0121	2.41E-10
800	0.0134	2.67E-10
900	0.0146	2.91E-10
1000	0.0148	2.95E-10
1100	0.0144	2.87E-10
1200	0.0136	2.71E-10

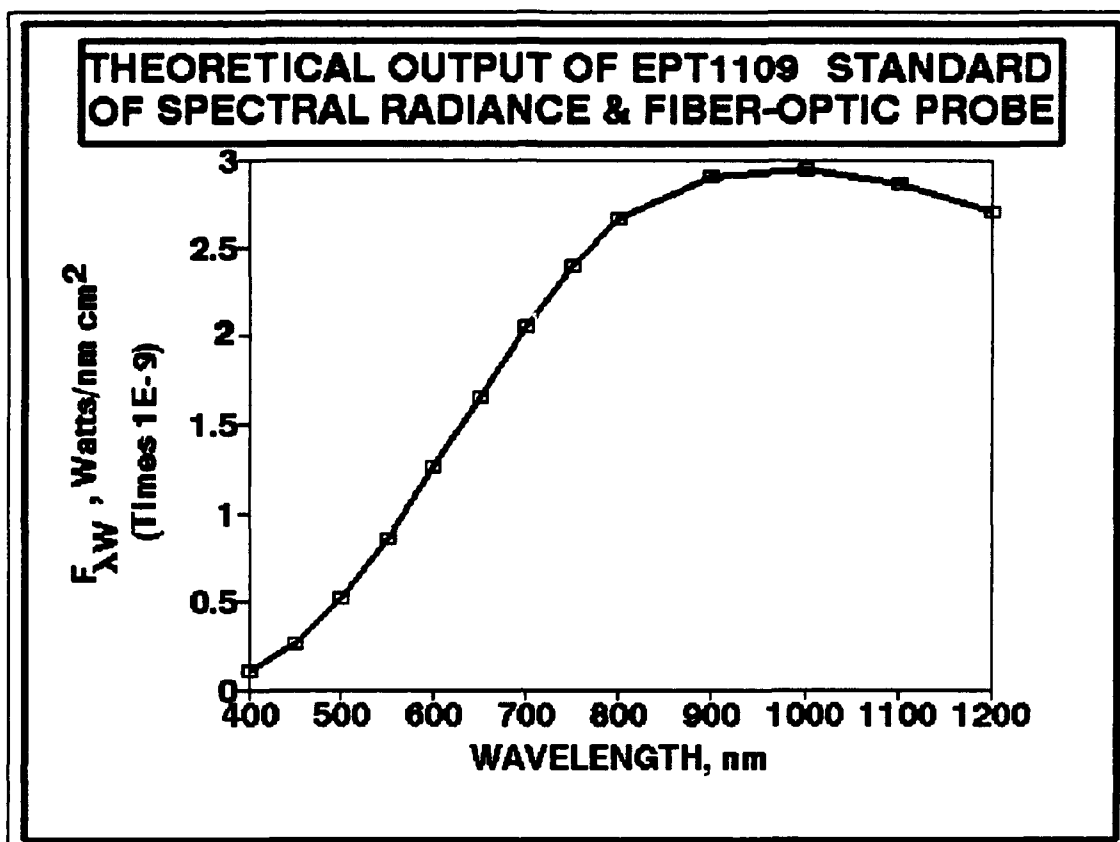


Figure 2.13: Plot of the Theoretical Output of EPT1109 Standard of Spectral Radiance and Fiber-Optic Probe at 100 cm Separation.

of different orders to this curve. A seventh order spline produced the best fit. Using this information with a locally produced program, called EQN, we calculated the coefficients for the seventh order polynomial equation describing the shelf standard source, serial number EPT-1109, behavior for the wavelength range of 400 nm to 1200 nm. Similar calculations were performed for a sample geometry with the fiber placed at 50 cm from the shelf standard source and with a diffuser in

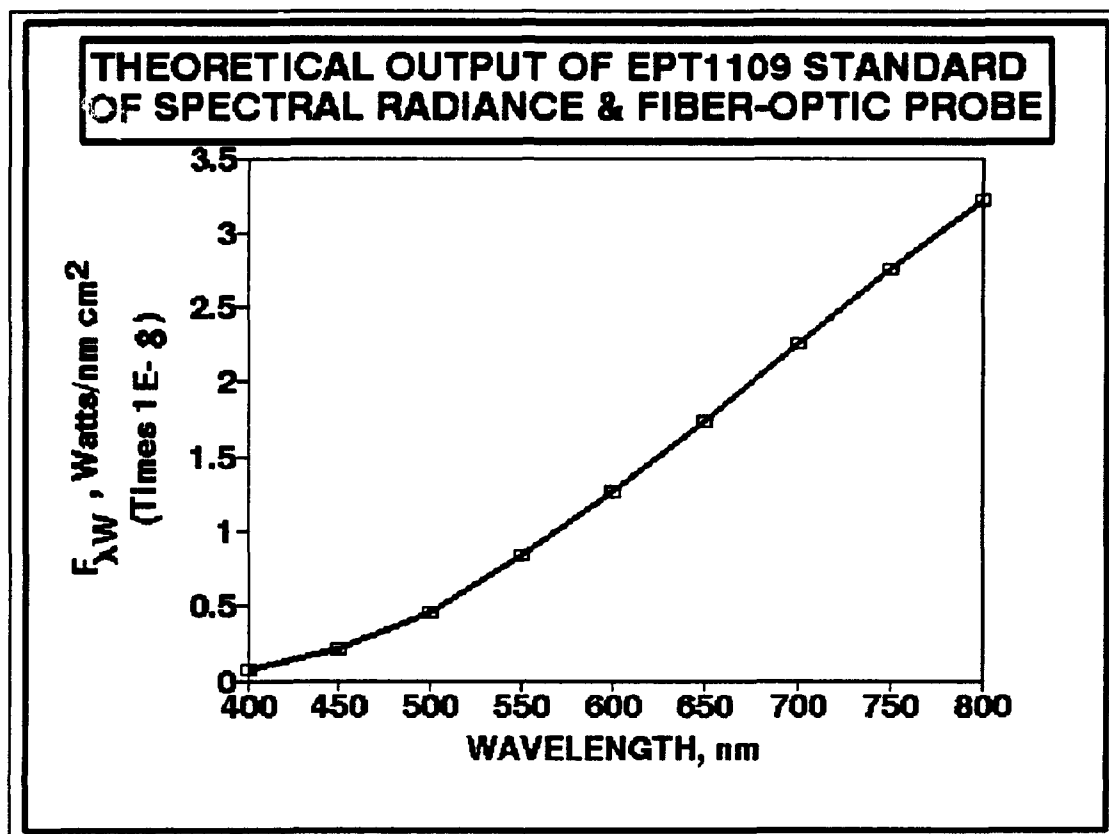


Figure 2.14: Plot of the Theoretical Output of EPT1109 Standard of Spectral Radiance and Fiber-Optic Probe (1x1) at 50 cm Separation.

the optical path. Figure 2.14 shows the theoretical output curve of the shelf standard white light source with the fiber-optic probe, when separated by 50 cm. Table 2.2 shows the calculations for this configuration. In this particular sampling geometry we limited the output calculation 400 nm to 800 nm because the transmittance of the diffuser is well known for that wavelength range.

Table 2.2: Theoretical Output of EPT1109 Standard of Spectral Radiance and Fiber-Optic Probe (1x1); 50 cm separation.

WVN	B_{λ}	$F_{\lambda W}$
400	0.000537	7.10E-11
450	0.00131	2.13E-10
500	0.0026	4.52E-10
550	0.00433	8.32E-10
600	0.00631	1.27E-09
650	0.00834	1.74E-09
700	0.0103	2.26E-09
750	0.0121	2.76E-09
800	0.0134	3.22E-09

2.4.2 White Light Source Holders

The holders for the white light sources are described in section 2.3.2 of and their importance in the sampling geometry control was discussed in section 2.2.1 of this paper. We experimented with several configurations for both white light source holders. Every configuration tested attempted to achieve reproducible intensity measurements by uniform illumination of the fiber-optic probe at the connection port of the holder. The holder for the laboratory working standard white light source was the first one to be developed. The initial models of this laboratory standard source holder included a disk with multiple apertures as a method of control of the radiance intensity reaching the fiber-optic probe. The disk have eight apertures from 0.0135" to 0.116". Figure 2.15

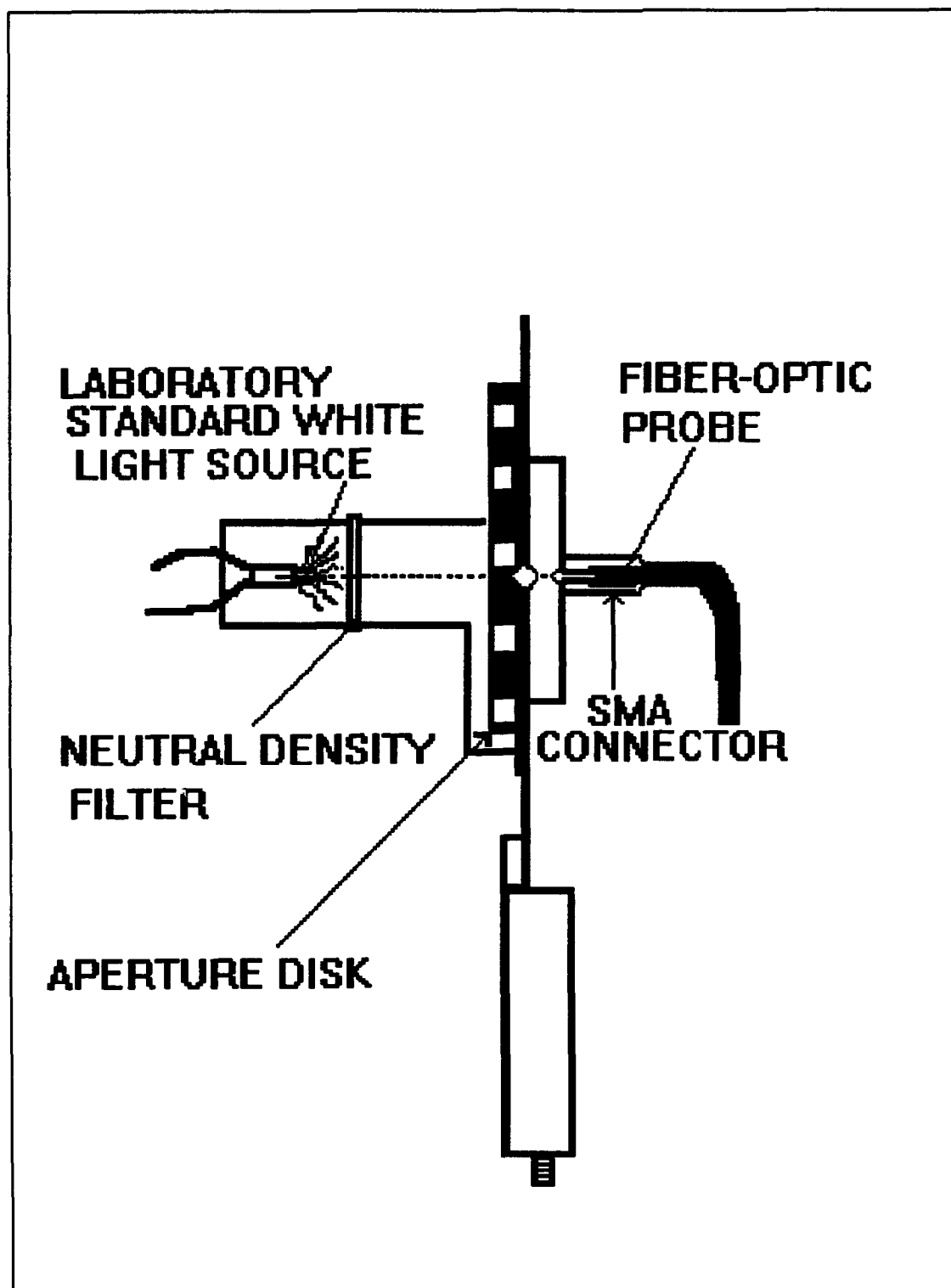


Figure 2.15: Initial Model of the Laboratory Standard White Light Source Holder.

shows the initial model of the laboratory standard source holder and the eight apertures dimensions. We found that apertures as small as 0.033" will introduce a diffraction pattern on the spectrum recorded from the laboratory working standard white light. This diffraction pattern cannot be eliminated by any possible correction, therefore invalidating the measurements. Other larger apertures worked well, but the presence of a disk with multiple apertures was introducing errors on the exact alignment of the center of the aperture with the source and the fiber-optic probe. Movement of the aperture disk caused by vibrations will introduce undesirable uncertainty on the uniform illumination of the fiber-optic probe. The latest version of the laboratory working standard white light source holder does not have a multiple aperture disk, but a fixed large aperture. This large aperture serves as a secondary radiant source that uniformly illuminates the extended tube that holds the connector for the fiber-optic probe. The extended tube that holds the fiber-optic probe arose from the need to reduce the intensity of the radiant energy collected by increasing the distance between source and collection fiber. A second function of this extended tube is to ensure uniform illumination of the collection fiber by avoiding angle sensitivity due to the close proximity of the fiber to the transmitting aperture. Angle sensitivity of the collection fiber could change dramatically the observed shape of the white light radiation collected from the source.

Therefore, it is extremely important that the holder for the laboratory standard white light source eliminate angle sensitivity in the collection fiber-optic by uniform and reproducible illumination.

The holder for the shelf standard white light source went through a series of systematic changes to ensure reproducible uniform illumination of the fiber-optic probe. One of the models more used in our research placed the fiber-optic probe at 50 cm from the tungsten ribbon of the shelf standard white light source. A diffuser made of white bond paper at 25.3 cm from the fiber-optic probe served as the intensity attenuator. Concerns with long-time effects of weathering in a paper filter and with the reproducibility of a replacement filter convinced us to try a system without a paper diffuser and with a longer distance between the fiber-optic probe and the spectral radiance source as a method of reducing the intensity of radiant energy collected at the fiber. The current working model does not use any diffuser between the collection optic and the source. Only neutral density filters are required to attenuate the intensity of the source reaching the collection fiber located 100 cm on direct line of sight with the tungsten ribbon. We found that this latest configuration not only produces reproducible uniform illumination of the fiber-optic probe, but also determine in a very simple way the area of the tungsten ribbon used. Because no intervening optics are used

between the collection fiber and the source, it is the solid angle of the fiber-optic that determine the effective area from the center of the tungsten ribbon that is imaged at the spectrometer. We also found out that using a black carton tube, large enough diameter (3") to avoid interferences with the optical axis, between the source and collection fiber reduces the amount of stray light or any type of spectral radiance that is not originated at the center of the tungsten ribbon and passed through the fused-silica window.

2.4.3 True Spectrum of the Laboratory Working Standard White Light Source

The determination of the true spectrum of the selected laboratory working standard white light and the calculation of the polynomial equation describing this behavior are fundamental steps of this research. This part of the process may appear trivial at first glance, but it involved the elucidation of several unsuspected relations between the responses of the system based on wavelength and pixel dependent parameters. The comparison of the output of two spectral radiance sources is a straight forward idea with rigorous experimental demands. We expected that the white light spectrum of the laboratory working standard white light source should be a smooth curve without major sudden changes on its intensity from one wavelength to the other. Our expectation comes from the well known fact that white light

shows a blackbody-like behavior. Our extensive experimentation of different configurations for sampling geometries, different fiber-optics and different CCD detectors revealed the following sources of artificial variations in the measurements of the outputs of both sources:

1. Small fluctuations of the current in the shelf standard source. Even variations of fractions of an ampere showed effects on the measured output of the shelf standard and its reproducibility.
2. Uneven illumination of the fiber-optic probe at the collection point. This effect was remarkably unforgiving at the configurations used for the laboratory working standard source. The smaller distance between the small bulb of the laboratory standard white light source and the collection fiber made critical that the connection for the fiber-optic probe must be very reproducible every time the fiber is connected back to measure the spectral radiance. Slight changes on the angle of illumination of the fiber-optic showed qualitative changes in the shape of the radiant output response and on the reproducibility of the intensity at the same window for a multiple operations of disconnecting and connecting back the collection

fiber to the source holder.

3. Changes in the transmission efficiency of the fiber-optic probes with changes in the radius of curvature of the fiber-optic probes. These changes may appear to be small, but they are amplified by any unsuspected excessive bending of the probe. Older fiber-optic probes demonstrated a higher trend to develop problems on this area. These fibers are more susceptible to damages. Even small damages to the fiber-optic probes will alter the reproducibility of the intensity measurement if the probe need to be removed and connected back for more measurements. The 1x6 fiber-optic probes showed greater problems in this area than the 1x1 fiber-optic probes.

The problems described above can be corrected or minimized by adjustments in the sampling geometry and experimental methods used to make the radiant output measurements of both sources. In section 2.3.3 we discussed two distinctive methods to measure the radiant output of both white light sources during calibration transfer experiments. The initial approach was to measure the output of each source within a given window before moving to the next one. This implies the switching of the fiber optic probe from one source to the other. The action of removing the fiber-optic probe

back and forth between the two white light source holders will introduce serious discrepancies in the intensities measured at the same wavelengths if the white light source holder does not provide either uniform illumination or reproducible positioning of the fiber-optic probe. A second approach was adopted to investigate this problem. This second approach assumed a small error on reproducing the position of the spectrometer grating through 12 spectral windows for two white light sources. We measured the radiant output of the 12 windows for one source before moving the fiber-optic probe to the next. The advantage of this method is that it ensures that no artificial changes in the intensities measured for the same wavelengths, at the overlapping boundaries of the windows, were introduced. The experimental set up that included a front-illuminated CCD and a shelf standard source holder with the fiber-optic probe at 50 cm from the source afforded good results in terms of a reduction in the intensity discrepancies for the same wavelengths measured in two adjacent windows. Intensity discrepancies between adjacent windows were reduced to the order of less than 1% standard deviation. The drawback of this method is that it does not simulate the actual procedures for measuring the output of the white light source prior to measuring the Raman spectrum of a sample. This is not a major problem as long as the artificial variations in the intensity measurements are removed before actual sample measurements are performed. The more serious problem with this

method arose when we used a more sensitive back-illuminated CCD detector in our system. The greater sensitivity of this detector showed large discrepancies in the intensities measured at overlapping wavelengths in adjacent windows. This problem was mainly caused by the lack of an exact pixel registration between the two white light sources. This lack of exact pixel registration also prevented a complete removal of pixel-to-pixel variation.

We concentrated our efforts on the experimental set up with the back-illuminated CCD (1024x1024) with a 1x1 Fiber-optic probe (400 micron) and the shelf standard source holder with the fiber-optic probe at 100 cm from the source. The output of both white light sources was measured for the 12 spectral windows of interest. Dark current spectra were subtracted from the corresponding white light spectra. We fitted a fourth order spline of zone length 1024 to each of the white light spectra of both sources on each window. The splines used were stiff because the information is not contained in random fluctuations of the spectrum but in the overall trend and shape of the curve. The spline provided us with a smoothed version of the spectral window. This curve give us the average intensity values for the pixels of the detector for any given window. These average values of intensity represent the best estimate of the true intensity of the source at any given pixel. A computer program, **EQN**, was

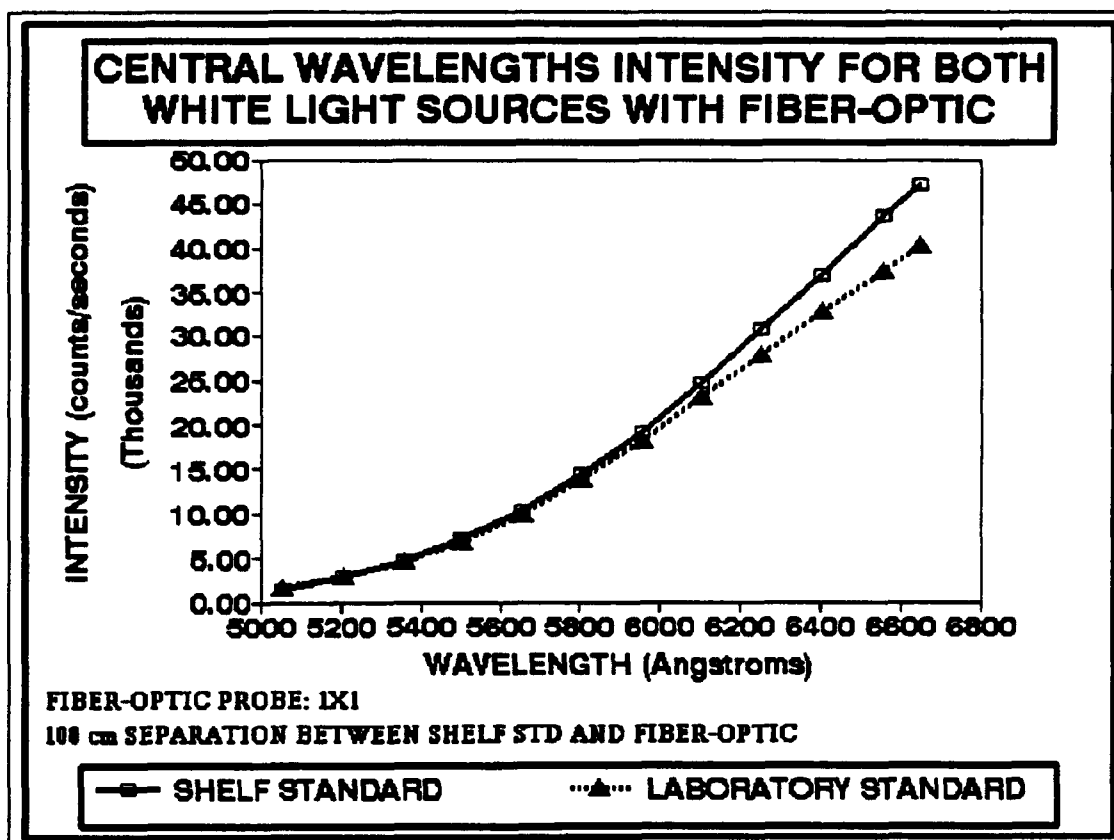


Figure 2.16: Plot of the Calculated Intensity for the Central Wavelength, in Counts/Seconds, of Each Window Versus Wavelength, in Angstroms.

used to calculate the coefficients of the fourth order polynomials describing the 12 spectral windows for each source. These coefficients were imported into a spreadsheet document to calculate the intensity of the central wavelength or pixel 511.5 of each window based in a fourth order polynomial. Figure 2.16 shows the plot of the calculated intensity, in counts/second, versus the central wavelength of each spectral window for both radiant sources. The intensity at the central wavelength of each window was essentially

calculated based on the experimental intensities of every single point in that particular spectral window. This central wavelength intensity represents the best estimate of the true trend of that spectral window. The robustness of this estimate is also increased by the fact that the central pixels of the detector offer the more unbiased response for the incident radiation.

The following calculations were based on the intensities calculated for the central wavelength of the spectral windows. First, we calculated the ratio of the intensity of the laboratory working standard white light source to the shelf standard white light source intensity for the central wavelength of each window. This ratio corrected the measurements by cancelling out the effects of instrumental artifacts in common to both sources in the experimental set up. At this point we used the calculated theoretical output of the shelf standard white light source with the fiber-optic probe, **SHELF $F_{\lambda w}$** , to determine the laboratory standard source's true output with the fiber-optic probe, **LAB $F_{\lambda w}$** . The seventh order polynomial equation describing the theoretical output of the shelf standard with the fiber-optic allowed us to calculate the corresponding intensity for each central wavelength. Multiplication of the calculated **SHELF $F_{\lambda w}$** by the calculated ratio of laboratory working standard to shelf standard white light source produced the desired **LAB $F_{\lambda w}$** for

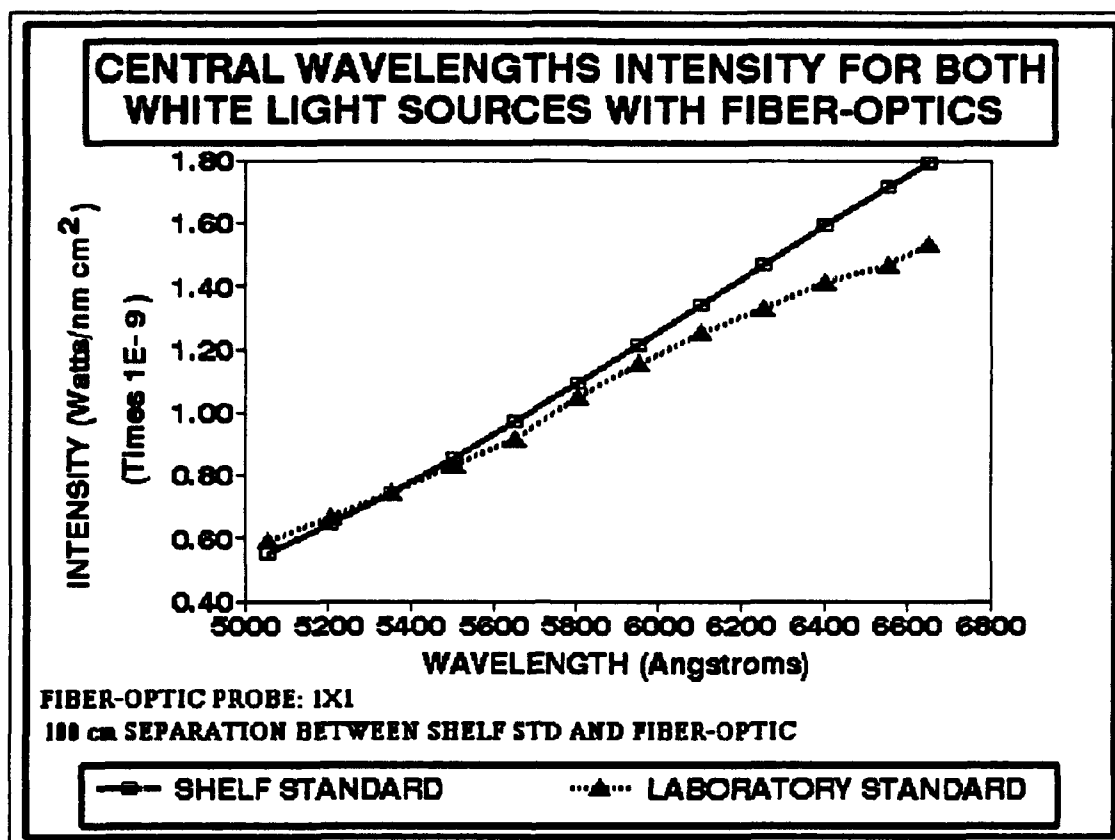


Figure 2.17: Plot of LAB $F_{\lambda W}$ and SHELF $F_{\lambda W}$ Versus Wavelength for the Central Wavelength of Each Window.

the central wavelength of each window. Figure 2.17 shows a plot of the LAB $F_{\lambda W}$ and the SHELF $F_{\lambda W}$ versus wavelength. The calculation of the output of the laboratory working standard white light source in photons/s nm, LAB $F_{\lambda P}$, was carried out by using the following equation:

$$\text{LAB } F_{\lambda P} = \text{LAB } F_{\lambda W} A_{\text{FIL}} \lambda_{\text{ctr}} (hc)^{-1} \quad (2.9)$$

where A_{FIL} is the area of the tungsten filament as described in

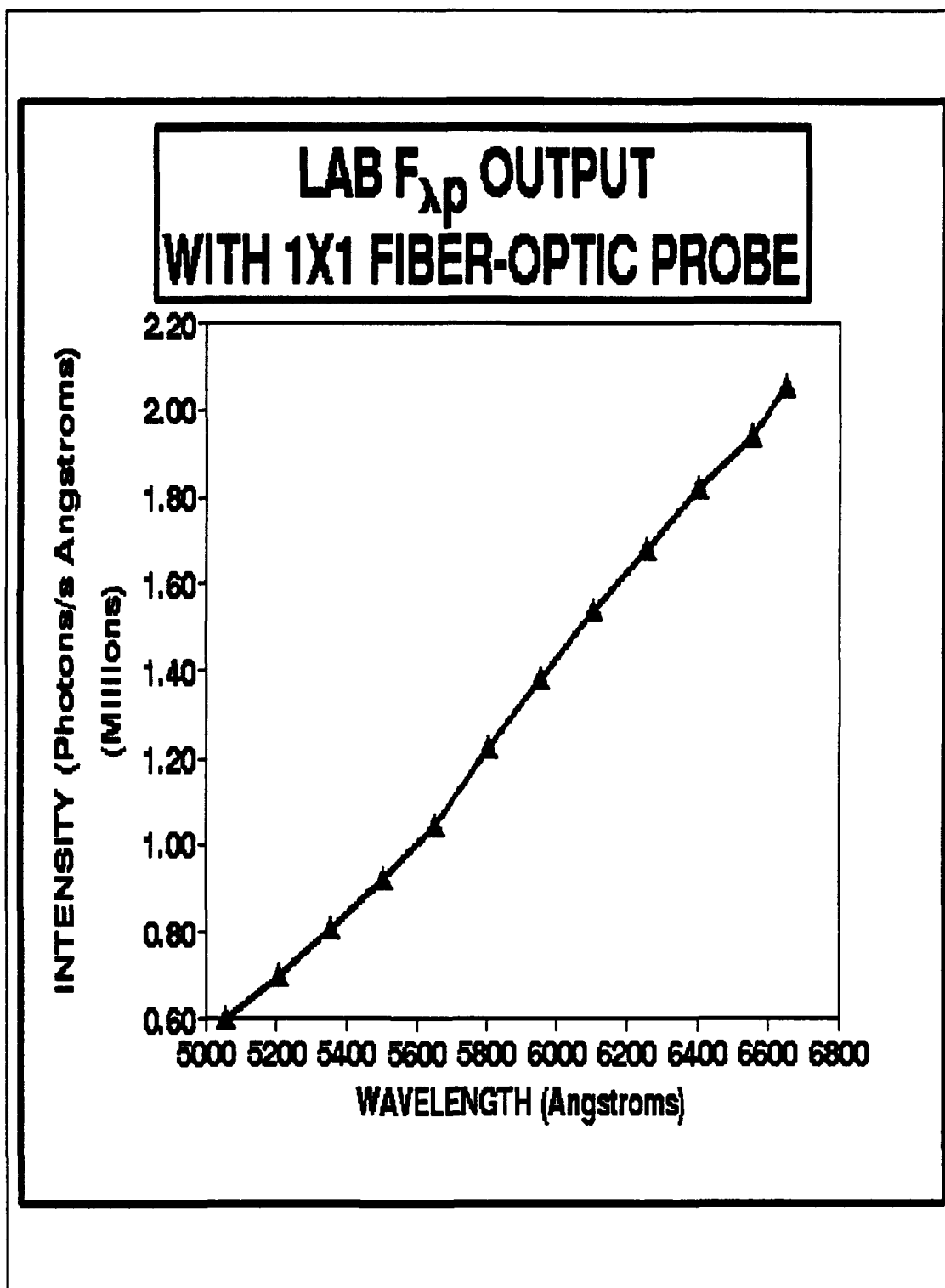


Figure 2.18: Plot of LAB $F_{\lambda p}$, in Photons/seconds Angstroms, Versus Wavelength.

Table 2.3: Coefficients for the Equation Describing the Curve LAB F_{λ} Versus λ .

Coefficients for the 6th Order Polynomial Describing the True Spectrum of the Laboratory Standard White Light Source in Photons s^{-1} (Angstroms) $^{-1}$:

A = 5.95E+05
B = 1.29E+03
C = -2.80E+00
D = 1.10E-02
E = -1.33E-05
F = 4.96E-09
G = 2.08E-13

section 2.2.5 and λ_{ctr} is the central wavelength. The plot and calculated coefficients for the polynomial equation describing the LAB F_{λ} are shown in Figure 2.18 and Table 2.3 respectively.

2.5 Conclusions

The purpose of the calibration transfer was to determine the "true spectrum" of the laboratory working standard white light source in units of photons/s nm. The simultaneous measurements of the outputs of the laboratory working standard and the shelf standards white light sources within a defined sampling geometry with a fiber-optic probe based system produced the required data to determine the true spectrum of the laboratory standard source. This method is straight

forward conceptually but demands excellent control and minimization of artificial sources of intensity variations in the measurements of the white light lamps. Uniform illumination, reproducible positioning of the fiber-optic probe at the collection ports, and a defined sampling geometry are essential elements in order to transfer the calibration from the shelf standard white light source to the laboratory working standard white light source. The data treatment procedures must provide the opportunity to eliminate the artifacts and the influence of parameters with dependencies on wavelength and pixel position as long as they are in common to both sources. The use of calculated intensities for the central wavelength of each spectral window to perform the calculations of the true spectrum of the laboratory standard white light source eliminated several discrepancies caused by differences of quantum efficiency of the detectors in its different pixels. The central wavelength intensities were based on the trends of all the points of each window.

The equations derived for the laboratory working standard white light source will serve as the bases of the calculation of the correction factor to be used for sensitivity corrections in real samples.

CHAPTER 3

SENSITIVITY CORRECTION FOR MULTICHANNEL SPECTROMETERS

3.1 Introduction

The main purpose of this research project is to develop a reliable method of correction for sensitivity variations in Raman systems that use multichannel spectrometers and array detectors. This correction method must correct the variations in sensitivity within a spectral window and interwindows. The eventual application of this correction method is to allow us to connect several spectral windows in order to obtain the complete Raman spectrum of the sample of interest in the given wavenumber range. The connections between the adjacent spectral windows should be smooth. Furthermore, the intensity ratios between the spectral features in different windows should be as significant as that existing for features within the same window. A detailed discussion of the theoretical aspects of the standard method for sensitivity correction and development of a new method was presented in **Chapter 1** of this paper. The following discussion will target the experimental

development and testing of a correction method for sensitivity variation by using a calibrated laboratory working standard white light source. These procedures are the follow up steps to the calibration transfer from the NIST standard to the laboratory working standard white light source.

3.2 Experimental

3.2.1 Outline of Experimental Procedure

The application of the sensitivity correction to samples involves three simple steps.

1. Calculation of the true output response of the Laboratory Standard Working white light source with the fiber-optic probe for the spectral window of interest.
2. Divide the sample spectrum by the measured spectrum for the Laboratory Working Standard white light source. Both spectra must be measured under the same conditions.
3. Multiply the ratio of sample spectrum to Laboratory Working Standard white light by the calculated true output of the Laboratory Working Standard white light for that window.

Three main tests can be performed to examine the effectiveness of the sensitivity correction method just outlined above. The first test involves the measurement of a sample spectrum, such as acetonitrile; correct its raw spectra for all windows in the wavenumber range of interest. Compare the ratio of peak intensities of the complete spectrum for the

compound, after catenation of the appropriate number of spectral windows, with the ratio of intensities observed for the same compound in an FT Raman spectrum. These ratios should be similar for the same features. The second test will require the measurement of the same sample at two different excitation wavelengths, and sensitivity correction with white light of both spectra. The correction with white light should successfully afford the same spectral shapes and intensities for both spectra. The third possible test is more complicated than the two just mentioned. For this third test we will measure the fluorescence spectrum of Quinine; correct it with the white light spectrum and compare it with the reported spectrum in the literature.

3.2.2 Sample Materials

Analytes in this research were acetonitrile (Methyl Cyanide) and Quinine Sulfate $[(C_{20}H_{24}N_2O_2)_2H_2SO_4 \cdot 2H_2O]$. Acetonitrile was supplied by Fisher Scientific (Fair Lane, New Jersey 07410) and used as received. Quinine sulfate was supplied by Fisher Scientific and a 5×10^{-5} M solution in H_2SO_4 (1N) was prepared for the actual measurements.

3.2.3 Instrumentation

The dispersive Raman system with a 514.5 nm argon ion laser and bifurcated fiber-optic probes was described in section 2.3.2 of this paper. The first configuration included

a 1x6 bifurcated fiber-optic probe with the front-illuminated CCD. A chevron notch filter, produced by the Omega Optical, INC, was used to reject the Rayleigh scattering in the path of the collimated beam. The second configuration used a 1x1 bifurcated fiber-optic probe with a back-illuminated CCD. A holographic notch filter purchased from Kaiser Optical Systems, INC. (371 Parkland Plaza, P.O. Box 983, Ann Arbor, MI 48106) was used to reject the Rayleigh scattering in this configuration.

A Varian Spectrofluorometer, model SF 330, with a Xenon

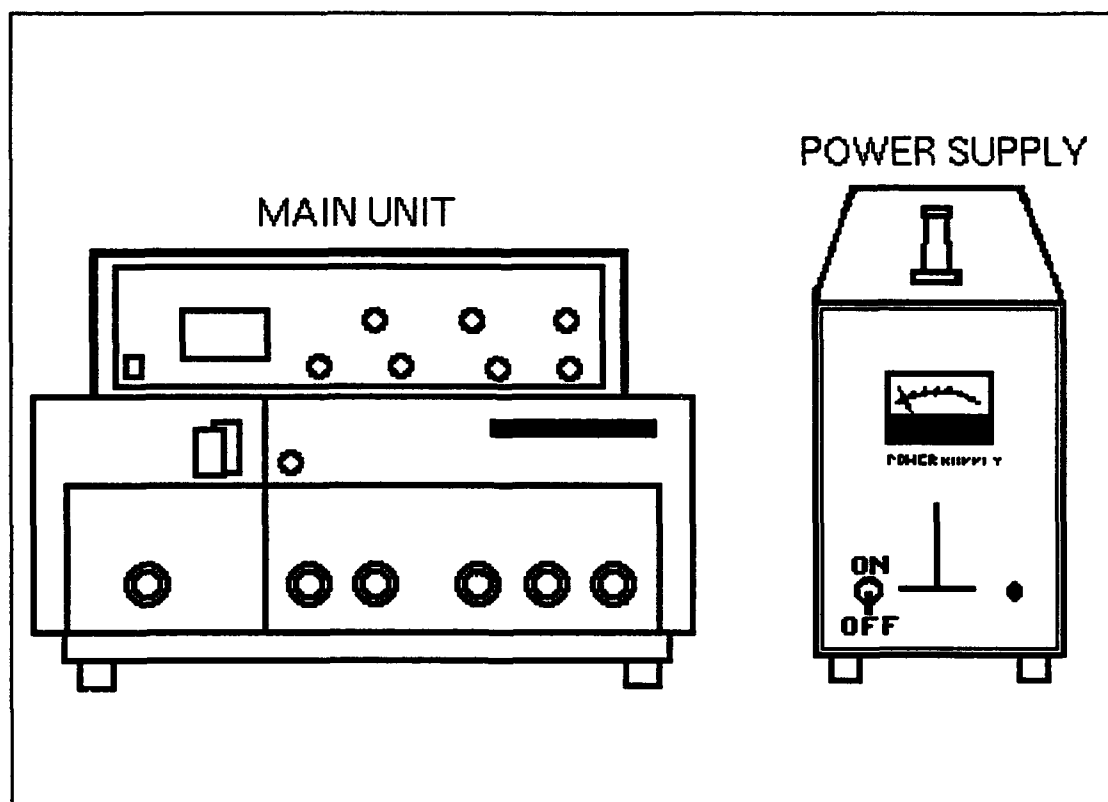


Figure 3.1: Varian Spectrofluorometer, SF330.

lamp was used to excite the Quinine solution at 345 nm. Figure 3.1 shows a diagram of the spectrofluorometer. A Welch-Allyn tungsten/halogen lamp, model 998418, was used as the Laboratory Working Standard white light source. A locally produced white light source holder was used to measure the white light spectra.

3.2.4 Measurements

All white light spectra were recorded at 1 second exposure time. A total of 100 replicas were coadded for the white light spectra recorded for the acetonitrile experiment. For the Quinine experiment, only 10 replicas were coadded.

The spectra for acetonitrile were recorded by coadding 40 replicas of 5 seconds exposure time each. A total of seven spectral windows were measured to cover the complete range of interest (525nm to 618nm) of the Raman spectrum of acetonitrile.

Fluorescence spectra of Quinine were recorded for seven spectral windows. For each window we recorded one replica, at 360 seconds exposure time each. The fiber-optic probe was placed inside the fluorescence cuvette, without contact with the Quinine solution as shown in Figure 3.2.

Dark current spectra were recorded for each sample and

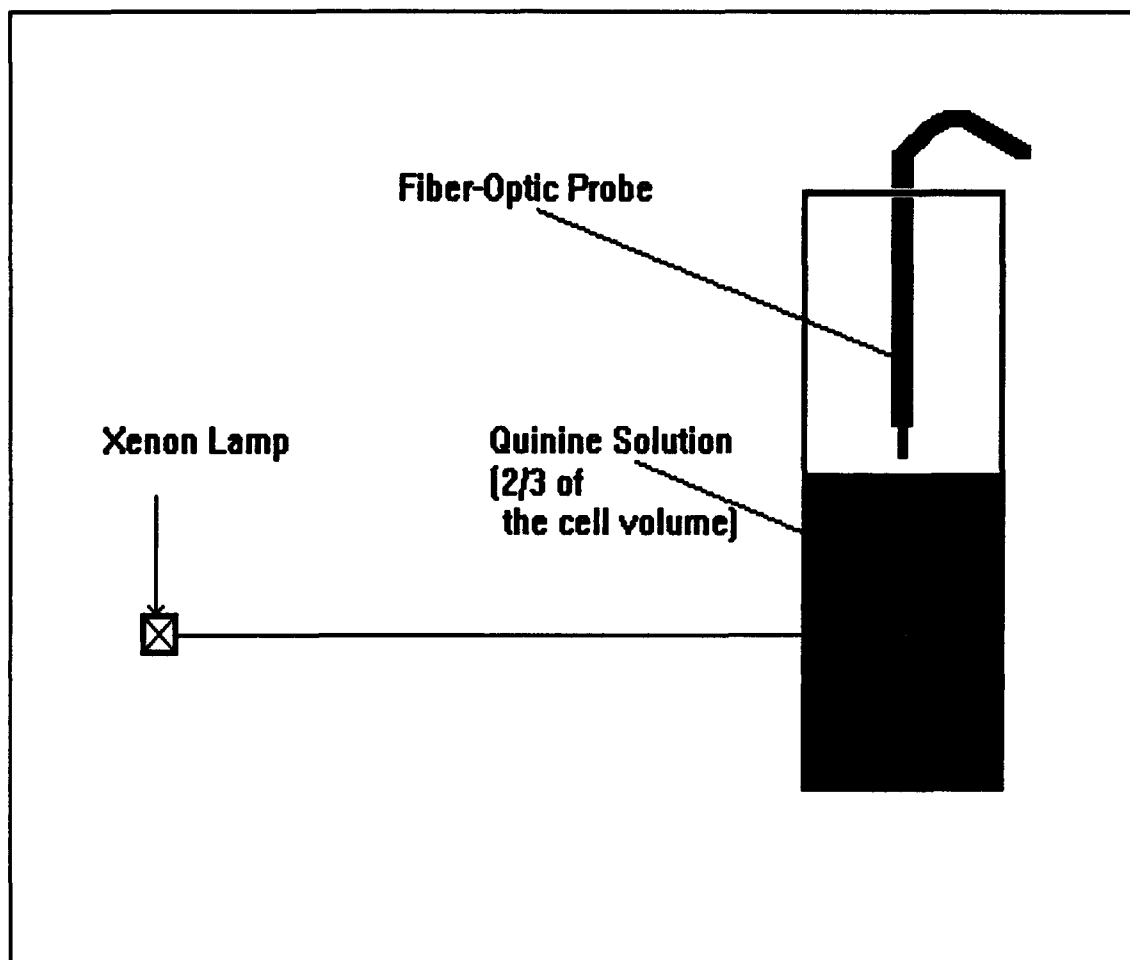


Figure 3.2: Experimental Arrangement for the Measurement of the Quinine Fluorescence Spectrum with a Fiber-Optic Probe.

white light spectra at the corresponding exposure time.

3.3 Results and Discussion

3.3.1 Acetonitrile Tests

The application of the sensitivity correction or white light correction to the spectra of all windows of acetonitrile

showed that the correction is noticeable in the relative intensities of the peaks as well as on the baseline of the spectra. We calculated the true output of the laboratory standard white light source with the fiber-optic probe, $F_{\lambda p}$, in photons $(s \text{ A}^\circ)^{-1}$, using the 7th order polynomial equation calculated in chapter 2 of this work. This calculation was performed for each window of interest. Using a simple spreadsheet document, we multiplied $F_{\lambda p}$ by the dispersion for each window in $\text{A}^\circ/\text{pixel}$, obtaining the $F_{\lambda p}$ in photons $s^{-1} \text{ pixel}^{-1}$ for 1024 points to create a binary set spectrum. Figure 3.3

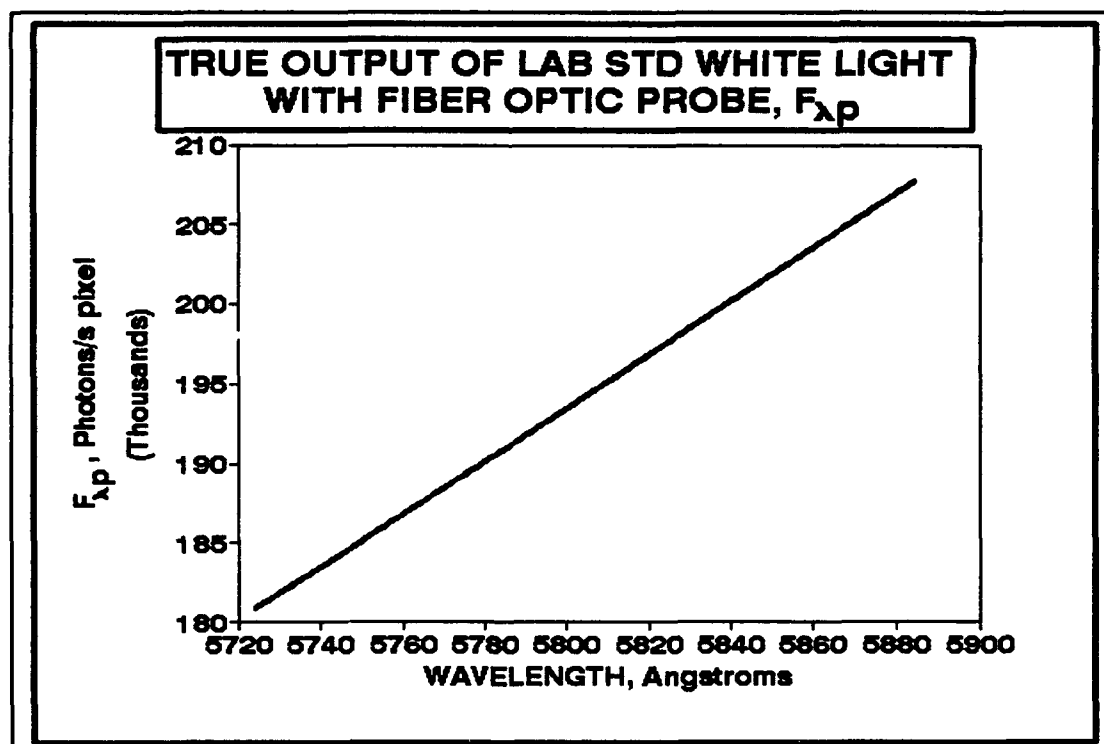


Figure 3.3: True Output of the Laboratory Standard White Light Source with the 1x1 Fiber-Optic Probe.

shows an example of the resulting curve for the wavelength range 5724.1 Å to 5884.8 Å.

We subtracted the dark current spectra from the measured spectra of the white light, acetonitrile and KCl (Silica background of the fiber-optic probe). The dark current corrected spectra of acetonitrile and KCl were divided by their respective exposure time (scaling) in order to obtain the intensity in terms of counts per seconds. The next step is to apply the critical white light correction, as described in

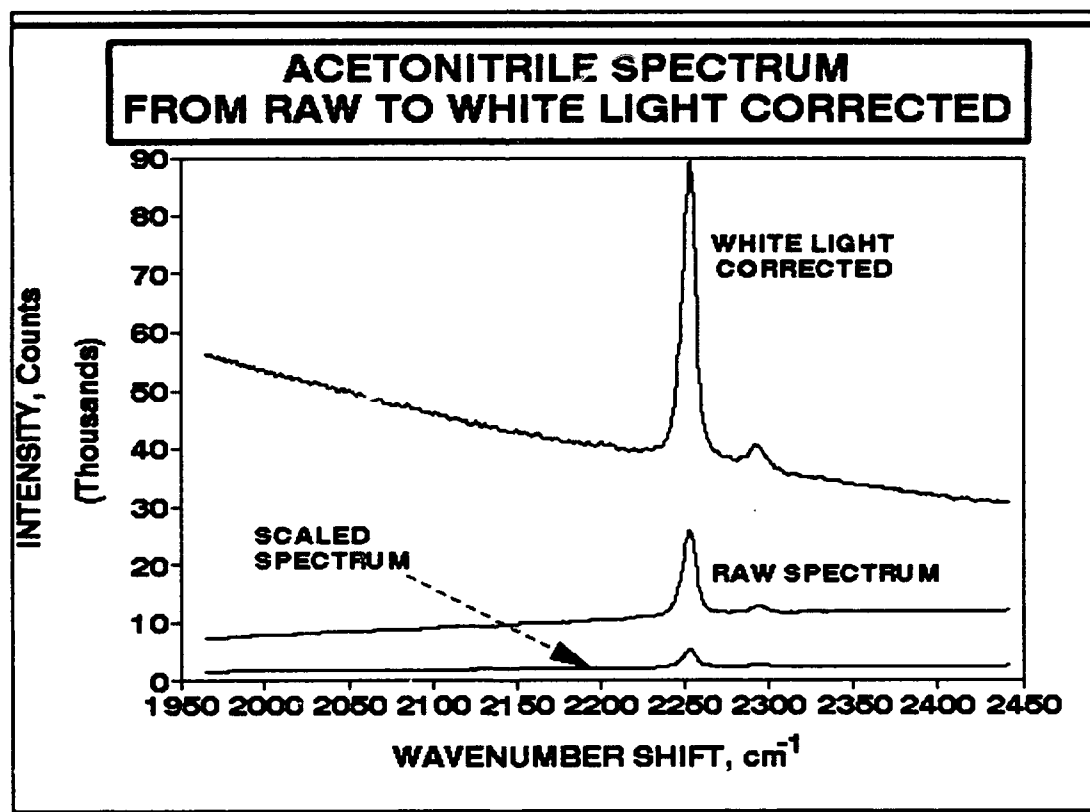


Figure 3.4: Acetonitrile Spectrum, Window 6, from Raw to White Light Corrected Spectrum.

section 3.2.1 to both acetonitrile and KCl. The resulting acetonitrile spectrum for window 6 (5723.8142A° to 5881.5267A°) are shown in Figure 3.4. Notice the large change on the intensity and the baseline of the spectra.

We decided to calculate the ratio of intensities of acetonitrile peaks in three different spectral regions. These regions are easily referred to as window 3 (central wavelength: 5354.59 A°), window 6 (central wavelength: 5804.53 A°), and window 8 (central wavelength: 6104.49 A°). We compared the peak ratios obtained for the dispersive Raman system (Argon ion laser, $\lambda_{exc} = 514.5$ nm) with those obtained from the FT-Raman system. Before we can calculate these peak ratios for the dispersive system, we must subtract the background spectrum of the fiber-optic probe (represented by KCl spectrum) from the white light corrected spectrum of acetonitrile for the windows of interest. Figure 3.5 shows the result of interactive subtraction of the KCl spectrum from the acetonitrile spectrum for the spectral window of 5724.1 A° to 5884.8 A°. The FT-Raman spectrum of acetonitrile is shown in

Table 3.1: Spectral Windows For Peak Ratios of Acetonitrile.

WINDOW	CWVL (A°)	$\Delta\delta$ (cm ⁻¹)
3	5354.59	760.78
6	5804.53	2208.42
8	6104.49	3054.96

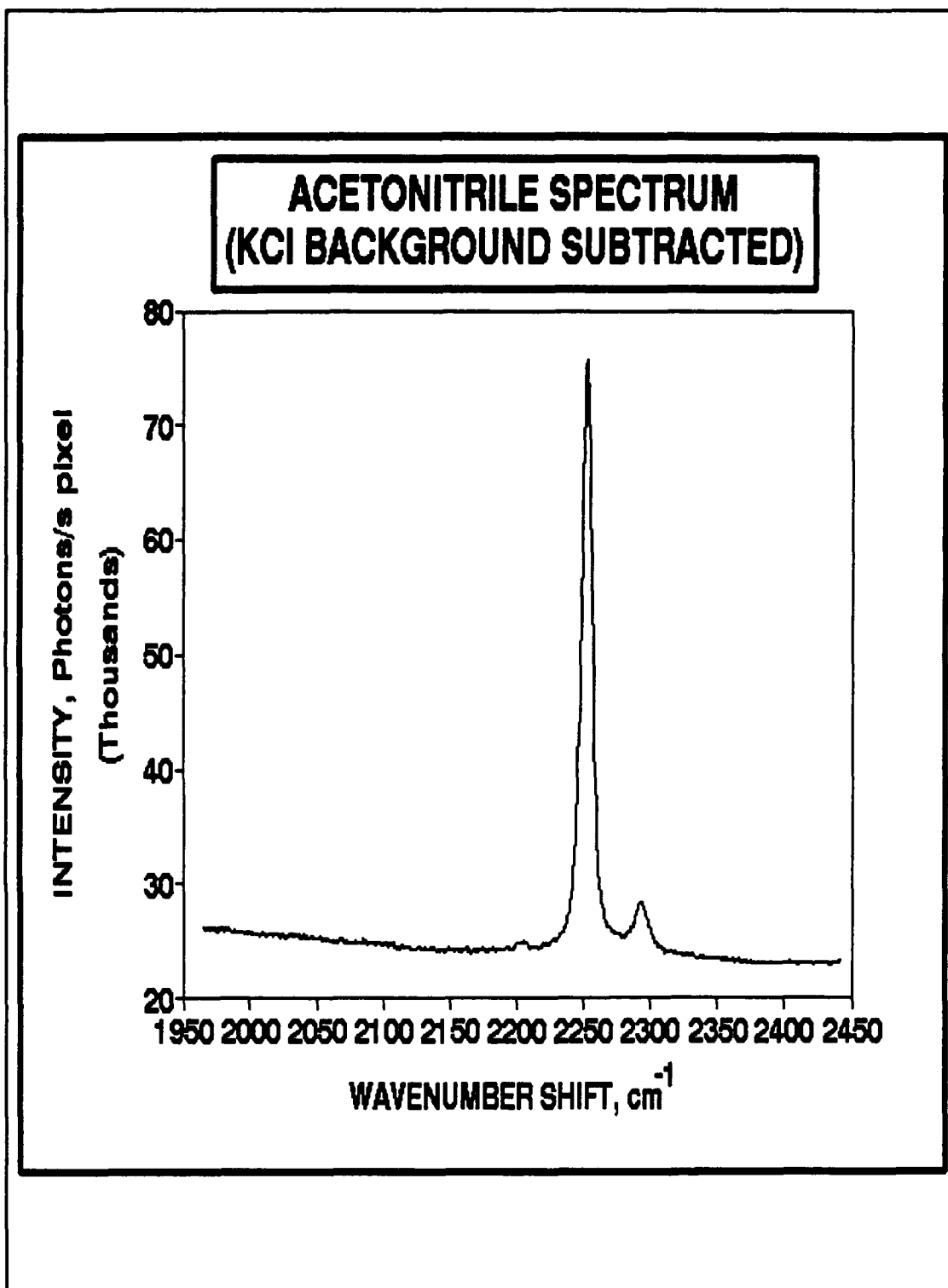


Figure 3.5: Acetonitrile Spectrum After Subtraction of KCl Spectrum; Window 6.

Figure 3.6; the three peaks of interest are labeled as window 3, window 6, and window 8. Table 3.1 shows the central wavelengths and corresponding wavenumber shifts for these windows.

Table 3.2: Results From Peak Intensity Ratio Comparison Between Dispersive Raman With and Without White Light Correction and FT-Raman.

PEAK RATIO	DISPERSIVE WITHOUT WL CORRECTION	DISPERSIVE WITH WL CORRECTION	FT RATIO
WIN8/WIN6	1.82	2.28	1.57
WIN8/WIN3	7.51	2.77	2.74
WIN6/WIN3	4.14	1.23	1.75

We measured the peak height, subtracted the baseline value and used this result as the maximum intensity of the acetonitrile peaks in windows 3, 6, and 8 for both the dispersive and FT Raman systems. The results of these calculation are shown in Table 3.2.

The FT-Raman spectrum is corrected by white light at once

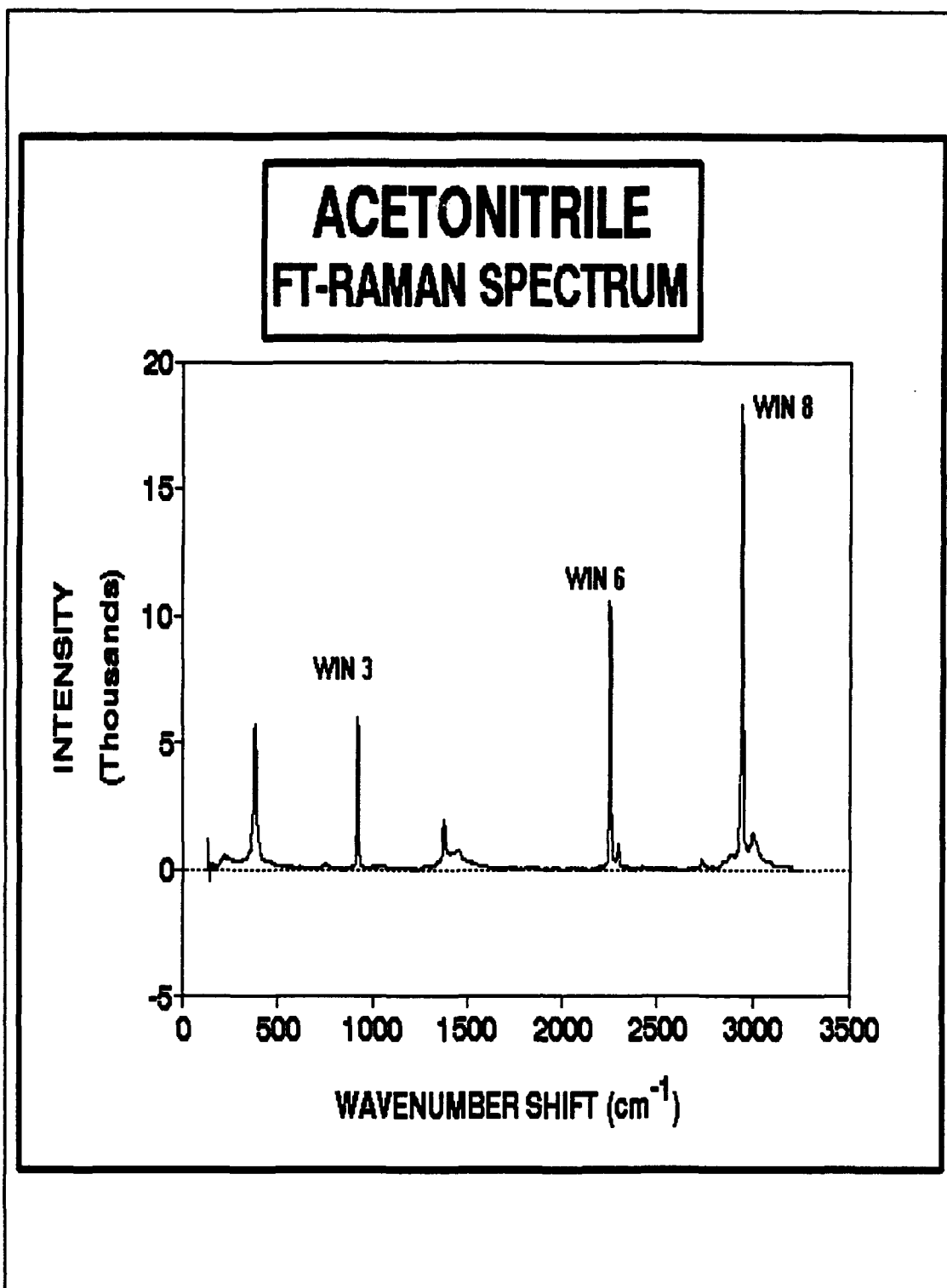


Figure 3.6: Acetonitrile FT-Raman Spectrum.

for all the peaks of interest in that spectral region. Therefore, it is reasonable to assume that the peaks intensity ratio in the FT-Raman spectrum will be close to the ratio of absolute intensities of the peaks in different windows of the white light corrected spectrum of the dispersive system. Nevertheless, we cannot assume that the white light correction of the FT-Raman is the best but at least it is standard to all the peaks in the spectral range of interest. Table 3.2 compares the results of the peaks intensity ratios for the FT-Raman with the peak ratio calculated for the dispersive with and without white light correction. The white light corrected peak ratio is an improvement in two out of three peak ratios calculated for acetonitrile. The best intensity ratio, compared to the FT-Raman values, for the dispersive spectra without white light correction was the ratio win8/win6, exactly the worst value for the ratio of intensities calculated for the white light corrected dispersive spectra. Contrary to this result was the comparison of the peaks at the extremes of the acetonitrile spectrum. The peak ratio of win8/win3, high wavenumber shift over low wavenumber shift, afforded the best result for the dispersive spectra corrected by white light. An important point is that the region where window 3 lies has a large signal of silica (KCl) background from the fiber-optic probe. The region of windows 6 and 8 does not have such a high silica background. These facts suggest that the white light correction is of critical importance when

comparing intensities of peaks at the extremes of the spectrum. These results indicate that the new white light correction is working to certain extent, but more refinement is required in the following areas.

1. The equation used to calculate the true spectrum of the white light response with the fiber-optic probe, $F_{\lambda p}$.
2. Subtraction of the silica background of the fiber-optic probe from the spectrum of the analyte of interest. This is done by interactive subtraction, which is a subjective process to the extent of the achievement of the best baseline of the resulting spectrum.
3. Accuracy of the FT-Raman white light correction.

These areas of concern will give us a better idea of what could be unreliable in the complete process of white light correction. The comparison of the dispersive system against the FT-Raman is a fast approach to identify and refine faults in the correction method that has been developed. Although the preliminary results of this test with acetonitrile are not conclusive in favor of the white light correction method, they indicate a good degree of success in the difficult task of

intensity correction for spectral features in different windows of the analyte of interest.

3.3.2 Quinine Fluorescence Spectrum Test

The quinine fluorescence spectrum was measured for seven spectral windows covering a range from 4942 Å ($20,234\text{ cm}^{-1}$) to 5978 Å ($16,728\text{ cm}^{-1}$) approximately. Both, quinine and measured white light, spectra were corrected for dark current. The theoretical response of the white light with the fiber-optic probe for each window was calculated using the 6th order polynomial equation describing it. We used these theoretical white light spectra to correct the quinine spectrum of each window.

The task of calculating the fluorescence spectrum of quinine for the whole range of wavelengths covered by the seven spectral windows is a very demanding task. Our approach was to fit a spline of 6th order with a zone length of 1024 points to each white light corrected spectrum of the seven measured windows of the quinine spectrum. From these splines we obtained the value for the central wavelength of each window. Using these intensity values for the central wavelengths and a locally produced program, **Bicubic Spline (BCS)**, we generated a 1024 points set representing the quinine spectrum for the wavelength (and wavenumber) region of interest. Figure 3.7 shows the calculated fluorescence

QUININE FLUORESCENCE SPECTRUM

BASED ON SPLINES INTENSITIES

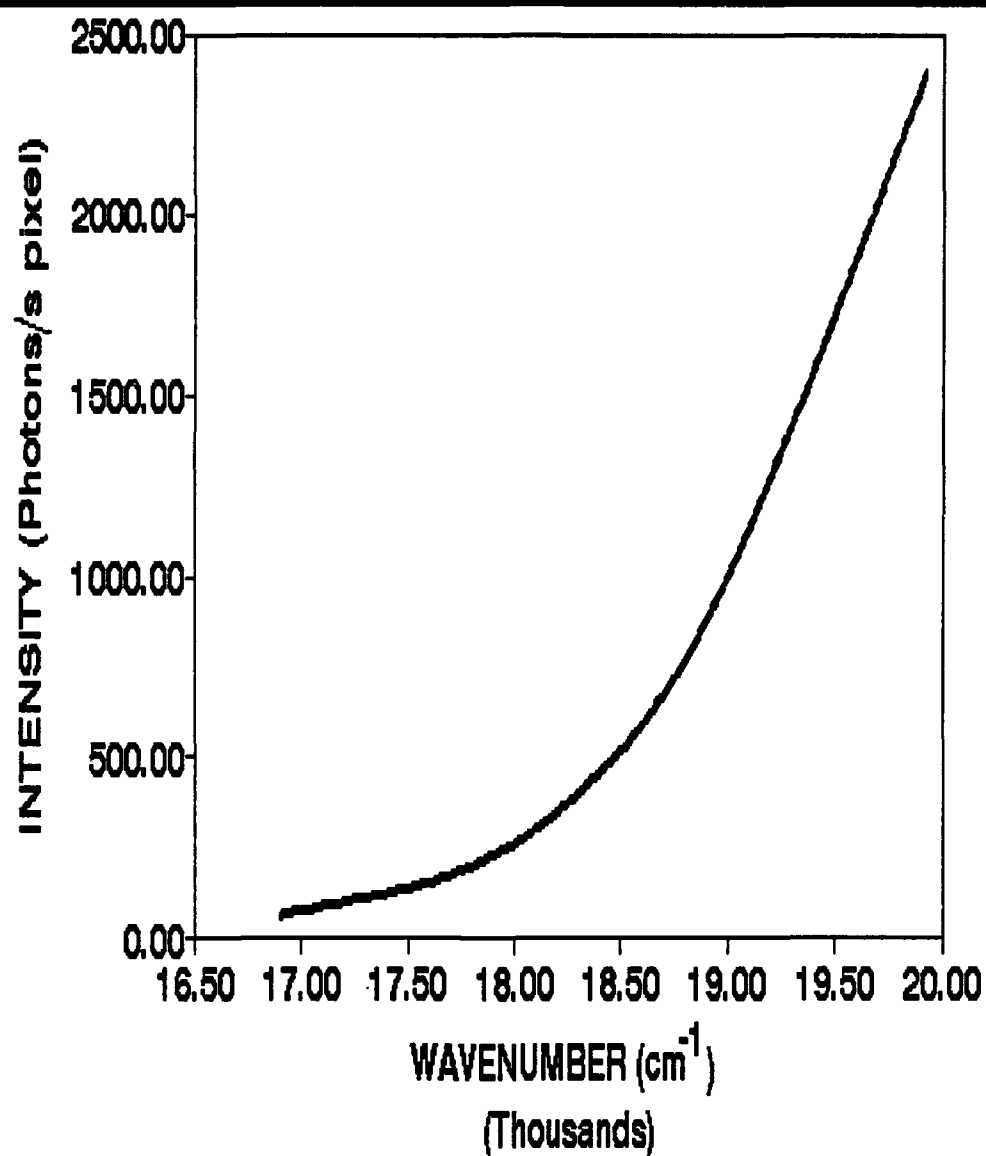


Figure 3.7: Quinine Fluorescence Spectrum Based on Splines Intensities.

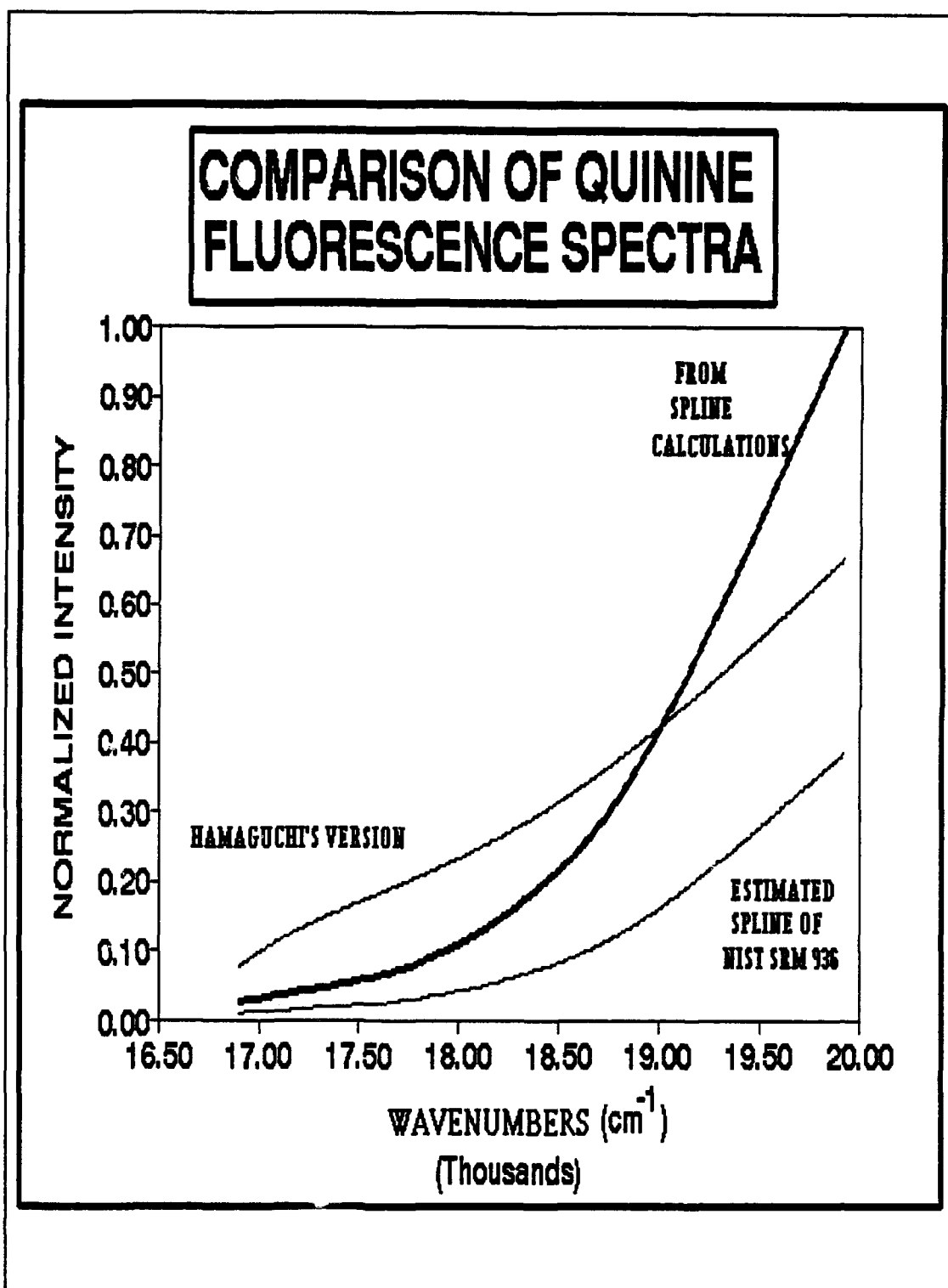


Figure 3.8: Comparison of Quinine Fluorescence Spectra; Spline Calculations, Hamaguchi's Version, and Spline of NIST SRM 936.

QUININE FLUORESCENCE SPECTRUM ACCORDING TO MELHUISH

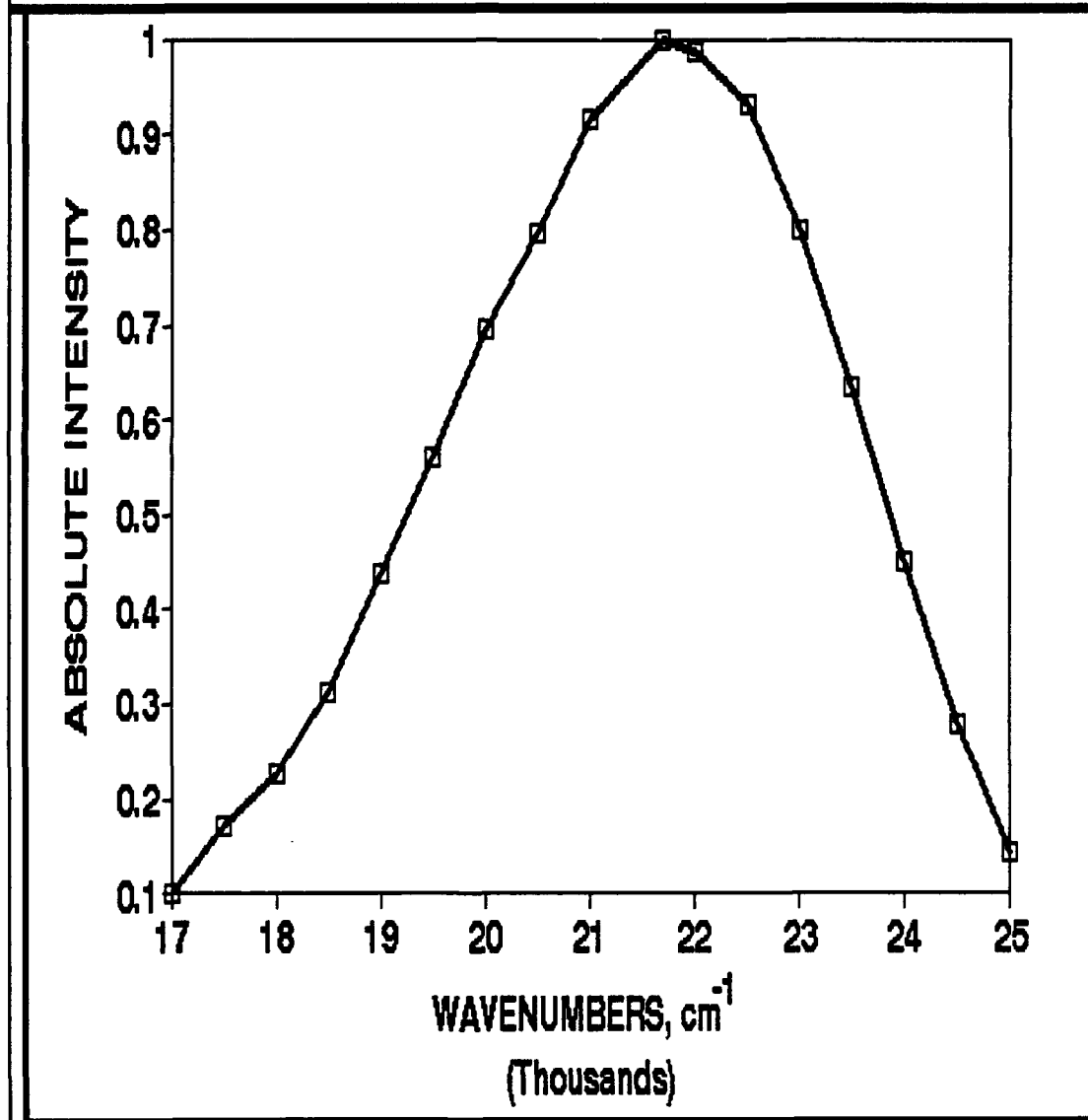


Figure 3.9: Quinine Fluorescence Spectrum According to W. H. Melhuish [10].

spectrum of quinine from $16,500\text{ cm}^{-1}$ to $20,000\text{ cm}^{-1}$. We compared the calculated fluorescence spectrum against the two of the quinine spectrum reported in the literature: Hamaguchi's [1] and the NIST SRM 936 [9]. Figure 3.8 shows this comparison. Our white light corrected fluorescence quinine spectrum is a smooth curve with fast changes of intensity values at the proximity of the high wavenumber region. This result has been reproducible with both CCD detectors, front and back illuminated. Nevertheless, the literature quinine spectra differ greatly from our white light corrected spectrum in the shape of the quinine spectrum at the high wavenumber region. The rate of change of the intensity with wavenumbers in the high wavenumber region is too fast in our white light corrected fluorescence spectrum. It is important to notice that Hamaguchi's quinine fluorescence spectrum has a slight bump in the region of $17,500\text{ cm}^{-1}$ and that the estimate for the NIST SRM 936 does not show this unusual feature, making it more similar to our white light corrected spectrum. The origin of this bump in Hamaguchi's quinine spectrum originates in the basic measurements performed by W.H. Melhuish [10] in 1975. Figure 3.9 shows the plot of the original 17 measurements of quinine intensity every 500 cm^{-1} . Despite this apparent difference, both spectra, Hamaguchi's and NIST SRM 936, compare very well in the high wavenumber region, where our white light corrected spectrum differs the most.

3.3.3 Conclusions

The differences and errors of our white light corrected quinine fluorescence spectrum in comparison with the reported spectra in the literature, point out some important areas for revision. First, we can clearly see that the high wavenumber region has been overcorrected by the present method for white light correction. The high wavenumber area is the region of less intensity measured at the calibration transfer of the shelf standard white light source to the laboratory working standard white light source. Furthermore, the sensitivity of the CCD detector is less in that region. These two factors combined could generate undesirable errors during the calibration transfer. Errors in that early stage of the process, although small, could propagate in potential larger errors by the time the white light correction is applied to the analyte of interest.

It is possible to introduce additional errors during the measurement of the intensity of the fluorescence radiation from quinine. Our set up for the experiment required us to use one fiber-optic probe to measure the white light, followed by quinine solution and finally the measurement of neon lines. This procedure involved, for each window, the movement of the fiber-optic probe from the white light source holder to fixed position with respect to the quinine solution and to a third set up for the neon lines measurements. The reproducibility of

the fiber-optic probe position with respect to the quinine solution, as it was shown in Figure 3.2, must be improved. This part of the procedure was of great concern at the time of experimental measurements. The results suggest that the control of the sampling geometry is essential to develop a common standard baseline for the intensity measurement of multiple spectral windows of a given analyte. Even slight changes in the separation distance and the orientation angle of the fiber-optic probe with respect to the quinine solution could cause large changes in the intensity collected at the probe.

The procedures to generate the equation to calculate the true white light spectrum of each spectral window must be reviewed for possible inconsistencies in the high wavenumber region. Additionally, the sampling geometry for the measurement of the fluorescence spectrum of quinine must be improved to the point where highly reproducible measurements can be performed for any given spectral window.

CHAPTER 4

GENERAL CONCLUSIONS AND RECOMMENDATIONS FOR THE INTENSITY CALIBRATION OF RAMAN MULTICHANNEL SPECTROMETERS

4.1 General Conclusions

Sensitivity variations in multichannel spectrometers require correction, better known as white light correction. The white light correction is of critical importance for the quantitative analysis of chemical analytes via multichannel Raman spectrometers. The general approach to transfer the calibration from the NIST Standard of Spectral Radiance to the laboratory working standard white light source is a feasible method , but it requires extremely good control of the sampling geometry. The method of changing the fiber-optic probe from one source holder to the other within any given spectral window is not a practical approach within the present constraints. This method fails to prevent changes on the exact position of the fiber-optic probe at the connectors of the white light source holders. For example, we noticed that SMA

connectors, with a 1x1 fiber, have a large effect on the intensity collected at the fiber-optic probe by just changing the tightness of the adjustment at the connector. Additionally, changes on the radius of curvature of the first 16 cm of the bifurcated fiber-optic probe caused severe changes in the intensity transmitted to the detector. These problems can be controlled for a given calibration experiment by using the method of measuring the intensity of one source for all spectral windows before measuring the next source. The error incurred on reproducing the spectrometer setting, therefore the grating position, for both white light sources will be smaller than the errors caused by the first method. Nevertheless, the method of measuring the radiance of all windows of one source before moving to the next, does not completely ensure reproducible intensity measurements. Changes in the radius of curvature of the fiber-optic probe and on the tightness of the SMA connector at the interface with the white light source holder will occur with extended period of time unless preventing measures are taken.

Small inconsistencies in the intensity measurements of the calibration transfer procedure will generate larger error in the eventual calculations for the determinations of the time spectrum of the laboratory standard white light source. The expected shape of the white light true spectrum for the laboratory standard should be very smooth curve without sudden

changes in the intensity with wavelength. This ideal curve cannot be achieved without the control and minimization of the problematic areas just mentioned above. Furthermore, the high wavenumber region of the white light spectrum is less intensive, causing inherent problems with sensitivity in addition to the already low sensitivity of the CCD detector in that region. Another point for revision is the validity of the calibration for the NBS Standard of Spectral Radiance, EPT-1109. The calibration must be current, otherwise we are risking the introduction of errors of considerable magnitude right from the most fundamental calculation leading to the effective calibration transfer and equation describing the true spectrum of the laboratory standard white light source.

The problems generated at the calibration transfer step of the intensity correction method will immediately show up on the application of the white light correction to chemical analytes. Overcompensation of sensitivity variations and intensity corrections are evident symptoms in some of our results. In addition to the problems with the calibration transfer, already discussed, the control of the sampling geometry of the analyte solution is a must. For both analytes tested, acetonitrile and quinine, it is of critical importance that the position of the fiber-optic probe be reproducible as accurate as possible from the intensity measurement at one spectral window to the next. Otherwise ,we are going to

compare the intensity of multiple windows, each with their own baseline intensity level due to the position of the fiber-optic probe. These problems, although they may look insignificant, could be the causes of larger errors at the time that the white light correction is applied.

In conclusion, the present approach for white light correction is working up to a reasonable extent. The failures in achieving more successful results, in the testing phase, lie on the demanding degree of control of the sampling geometry. Many of these small details were taken for granted as being compensated by the fiber-optic probes excellent properties. Before this work, these areas of problems were unknown. The following section discuss the lesson learned and suggestions to achieve a reliable and effective white light correction for multichannel spectrometers.

4.2 Recommendations

The following recommendations are geared to improve the reproducibility of the intensity measurements during the calibration transfer from the NIST Standard of Spectral Radiance to the laboratory working standard white light source.

1. Use a recently calibrated NIST Standard of Spectral Radiance source as the shelf standard lamp.

2. Develop a "key hole" SMA fiber optic connector for the white light source holder. This will lock the fiber in one position at the same distance and orientation with respect to the source in a reproducible manner.
3. Use of fiber-optic probe with a "metal jacket" in the first 16-20 cm of length from the excitation/collection end. This feature combined with any kind of clamps or holding devices to fix the radius of curvature of the fiber optic in a given position, without damage it, will ensure a consistent and reproducible transmission of collected radiation.
4. Use the method of measuring all spectral windows of a source before measuring the next. Eventually, this approach will be realistic even for actual sampling because dedicated fibers can be employed to measure white light only without the need of removing it.
5. Experiment with a single fiber-optic probe instead of 1x1 or 1x6 bifurcated bundles. A single fiber optic will serve as a simple light transmitter from the source to the collection optics at the

spectrometer. This approach could avoid some of the problems found with 1X1 and 1X6 fiber-optic probes. Low intensity collection from the source should not be a problem even with a single fiber-optic probe.

We have two major recommendations for the testing procedures with analytes.

1. Develop a "Key Hole" SMA connector system for the sample holder. The sample holder of fixed geometry is necessary to have consistent intensity measurements for multiple spectral windows and from one experiment to next in a testing series .
2. Adopt a system of with dedicated fiber-optic probes for the measurement of the analyte, for the white light and for the neon lines; a total of three separate fiber-optic probes. This will require individual alignment of each fiber with respect to the spectrometer, but it will maximize the reproducibility of intensity measurements for experiments with multiple windows and between experiments.

In summary, an extensive preliminary work on

identification of sources of variance and errors in the development of a reliable white light correction method for multichannel spectrometers have been performed. We developed a basic methodology combined with theoretical and practical principles to support further development of the present approach and its ultimate goals. The original goals of this project are within reach. Now, we have the bases to make the required adjustments, as recommended, and to conduct statistical analysis of a series of quantitative tests with a series of analytes and techniques.

REFERENCES

1. H. Hamaguchi, Appl. Spectrosc. Rev. **24**, 137 (1988).
2. C. Tseng, J.F. Ford, C.K. Mann and T.J. Vickers, Appl. Spectrosc. **47**, 1808 (1993).
3. M. Fryling, C.J. Frank and R.L. McCreery, Appl. Spectrosc. **47**, 1965 (1993).
4. R. Stair, R.G. Johnson and E.W. Halbach, J. Research NBS **64A**, 291 (1960).
5. The Eppley Laboratory, INC.; "Instructions for using Standards of Spectral Radiance" February 16, 1994.
6. J.D. Ingle, Jr. and S.R. Crouch, Spectrochemical Analysis (Prentice-Hall, INC., New Jersey, 1988), p.16-17, 59-60.
7. C.K. Chong, C. Shen, Y. Fong, J. Zhu, F.X. Yan, S. Brush, C.K. Mann, and T.J. Vickers, Vib. Spectrosc. **3**, 35 (1992).
8. M.L. Myrick, S.M. Angel, and R. Desiderio, Appl. Optics **29**, 1333 (1990).
9. J.W. Hofstraat and M.J. Latuhihin, Appl. Spectrosc. **48**, 436 (1994).
10. W.H. Melhuish, Appl. Opt **14**, 26 (1975).

Biographical Sketch

**Juan Ariel Cuadrado Reyes
Captain, Chemical Corps
United States Army**

Juan Ariel Cuadrado Reyes is a native of San Juan, Puerto Rico. He is married to the former Ada Nelia Medina Delgado and has two beautiful children, Ada Janet and Joseph Ariel.

His educational background includes undergraduate biomedical research and a B.S. in Industrial Chemistry from the University of Puerto Rico, Humacao Campus in 1985. He has the following U.S. Army Courses: Radiological Safety Course; U.S. Army Chemical School Instructor Training Course; Combined Arms and Service Staff Course at the U.S. Army Command and General Staff College; Chemical Officer Basic Course (Honor Graduate); Toxic Agent Training at the Live Agent Chemical Decontamination Facility, Fort McClellan, Alabama; Hazardous Waste Accumulation Site Manager Course; Chemical and Nuclear Weapons Targeting Course; Airborne School; Jumpmaster School; and Chemical Officer Advanced Course (Distinguished Honor Graduate).

Captain Cuadrado has served as a field artillery officer in the 2-162d Field Artillery Battalion of the Puerto Rico National Guard. During these years, he was also working as Chemist Supervisor in the Quality Assurance Division of ALUMEX Company, Canovanas, Puerto Rico until 1987. In 1987 he was ordered to active duty service as a battalion chemical officer for the 1-39 th Field Artillery Regiment (Airborne) at Fort Bragg, North Carolina. While brigade chemical officer of the 18 th Field Artillery Brigade (Airborne) at Fort Bragg, his unit deployed to Saudi Arabia and participated in Operations Desert Shield and Desert Storm. Upon returning from the Persian Gulf, Captain Cuadrado was assigned to Fort McClellan, Alabama, where he served as the Chief of Radiological Laboratories Edwin R. Bradley, and instructor of Chemical and Biological Warfare Defense at the U.S. Army Chemical School.

Upon completion of his Master's in Science at Florida State University, Captain Cuadrado will be assigned to the U.S. Army Military Academy, West Point, New York, as an Assistant Professor of Chemistry.